Marine Pollution Bulletin 170 (2021) 112536

Contents lists available at ScienceDirect

Marine Pollution Bulletin

journal homepage: www.elsevier.com/locate/marpolbul

Assessing the risk of light reduction from natural sediment resuspension events and dredging activities in an inshore turbid reef environment

Heidi M. Luter [a], Mari-Carmen Pineda [a], Gerard Ricardo [a], David S. Francis [b], Rebecca Fisher [a,c], Ross Jones [a,c,*]

[a] Australian Institute of Marine Science, Townsville, QLD and Perth, WA, Australia
[b] School of Life and Environmental Sciences, Deakin University, Geelong, VIC, Australia
[c] The UWA Oceans Institute University of Western Australia, WA, Australia

ARTICLE INFO

Keywords:
Turbidity
Light availability
Suspended sediments
Dredging
Corals
Bioeroding sponge

ABSTRACT

The reduction in benthic light from natural sediment resuspension events, dredging activities and clouds was quantified over multiple time periods (days to weeks) from a 3-year in-situ field study in the inshore turbid-zone coral communities of the Great Barrier Reef. The results were then used to examine the tolerance levels of three coral species and a sponge to light reduction and associated changes in spectral light quality (in conjunction with elevated sediment concentrations) in a 28-day laboratory-based study. All species survived the exposures but sub-lethal responses involving changes in pigmentation, lipids and lipid ratios were observed. A pocilloporid coral was the most sensitive taxon, with a 28-d EC10 value for bleaching (dissociation of the symbiosis) of 2.7 mol photons m^2 d^{-1}. The possibility of such light reduction levels occurring naturally and/or during maintenance dredging activities was then examined using the 3-year in-situ field study as part of a risk assessment.

1. Introduction

In shallow, coastal coral reef systems, elevated water cloudiness (turbidity) from natural wind and wave induced sediment resuspension events (Ogston et al., 2004; Orpin and Ridd, 2012), tidal resuspension events (Kleypas, 1996) and/or terrestrial run off (Fabricius, 2005; Guest et al., 2016; Rogers, 1990) is a very well-recognized hazard for benthic organisms. The light scattering and absorption by non-algal (mineral) particles alters benthic light quality (spectral composition) and quantity, limiting the ability of primary producers to assimilate energy through photosynthesis (Kirk, 2010; Mobley, 1994). Changes in benthic light availability is also a well-known hazard associated with dredging activities where sediments are released into the water column by disturbance of the seabed and by disposal at sea in dredge-material placement areas (Bak, 1978; Foster et al., 2010; Jones et al., 2016; Rogers, 1990).

Translating this hazard of elevated suspended sediment concentrations (SSCs) and changes in light to a risk is essential for management purposes. For dredging, it is an important part of the environmental impact assessment process (EPA, 2016; GBRMPA, 2012; Jones et al., 2016) and for developing water quality thresholds to manage dredging projects when underway. Recent studies during several large-scale capital dredging projects have shown that close to dredging there are occasions where sediment caused complete loss of all benthic light for up to several days, even in shallow (<10 m) tropical environments (Fisher et al., 2015; Jones et al., 2016; Jones et al., 2015). However, a more common occurrence was very low light (daytime *twilight* periods), which can occur for extended periods i.e. days to weeks. Suspended sediments also altered the underwater spectral profile, preferentially attenuating the more photosynthetically useful shorter bluer wavelengths of the visible/photosynthetically active radiation (PAR, 400–700 nm) spectrum (Fearns et al., 2019; Jones et al., 2016). Together with the preferential attenuation of red light with depth (Kirk, 2010; Smith and Baker, 1981), the nett effect of preferentially attenuating wavelengths at both ends of the PAR spectrum is a progressive monochromation of underwater light to yellow-green wavelengths at increased depth and increased SSC (Jones et al., 2016).

A number of recent laboratory-based experiments have examined the responses of corals and photosynthetic sponges to light reduction in association with sediments (Bessell-Browne et al., 2017a; Jones et al., 2020; Pineda et al., 2017a). When exposed to combinations of low light and elevated SSCs there were changes in total lipid levels and ratios of storage to structural lipid, and ultimately there was a sub-lethal

* Corresponding author at: Indian Ocean Marine Research Centre, Level 3, The University of Western Australia, Crawley, WA 6009, Australia.
E-mail address: r.jones@aims.gov.au (R. Jones).

https://doi.org/10.1016/j.marpolbul.2021.112536
Received 29 January 2021; Received in revised form 13 April 2021; Accepted 20 April 2021
Available online 11 June 2021
0025-326X/© 2021 Elsevier Ltd. All rights reserved.

dissociation of the coral-algal symbiosis i.e., bleaching (Bessell-Browne et al., 2017a; Bessell-Browne et al., 2017b; Jones et al., 2020). These laboratory based studies were conducted with corals collected from an offshore, *blue water*, low turbidity environment; however, many capital and maintenance dredging campaigns occur in inshore coastal areas near reefs where turbidity regimes (hence light availability) are highly variable (Larcombe et al., 1995).

In this study we continue the investigation of the longer-term effect of a decrease in light from elevated SSCs on benthic phototrophs but using corals collected from the *turbid coastal-zone reefs* (Larcombe and Woolfe, 1999; Woolfe and Larcombe, 1998; Woolfe and Larcombe, 1999) of the inshore central Great Barrier Reef (GBR) Marine Park (Done, 1982; Hopley et al., 1989). Light availability is already thought to be a limiting factor in these environments (Anthony and Connolly, 2004; Anthony et al., 2004; Morgan et al., 2016), and to frame the investigation we describe the results of a long-term light and turbidity water quality monitoring to characterise baseline conditions. The results were used in a 28-day laboratory-based study experiment to examine the tolerance levels of three coral species and a sponge to light reduction with associated changes in spectral light quality and in conjunction with elevated sediment concentrations. The results are discussed with respect to light-based thresholds for future dredging projects, but also low light periods caused by natural sediment resuspension events, and cloud cover in a turbid coastal-zone reef setting.

2. Methods

2.1. Field setting

The field component of this study was conducted in Cleveland Bay and on the reefs around Magnetic Island in the inner central GBR (Fig. 1). The area has been the subject of numerous studies associated with understanding sedimentary processes, transport and fate, and the effects of watershed development on reef growth in *marginal* (cf. Perry and Larcombe (2003)) environments (Browne, 2012; Browne et al., 2010, 2013; Browne et al., 2012; Carter et al., 1993; Larcombe et al., 2001; Larcombe et al., 1995; Macdonald et al., 2013; Orpin and Ridd, 2012; Orpin et al., 2004; Perry et al., 2012; Whinney et al., 2017).

The Bay is naturally very turbid (Larcombe et al., 2001; Larcombe et al., 1995; Orpin et al., 2004) with natural wind-wave conditions sufficient to resuspend bottom sediments at 5 m depth occurring on an estimated 220 days per year (Orpin et al., 1999). Tides are dominantly

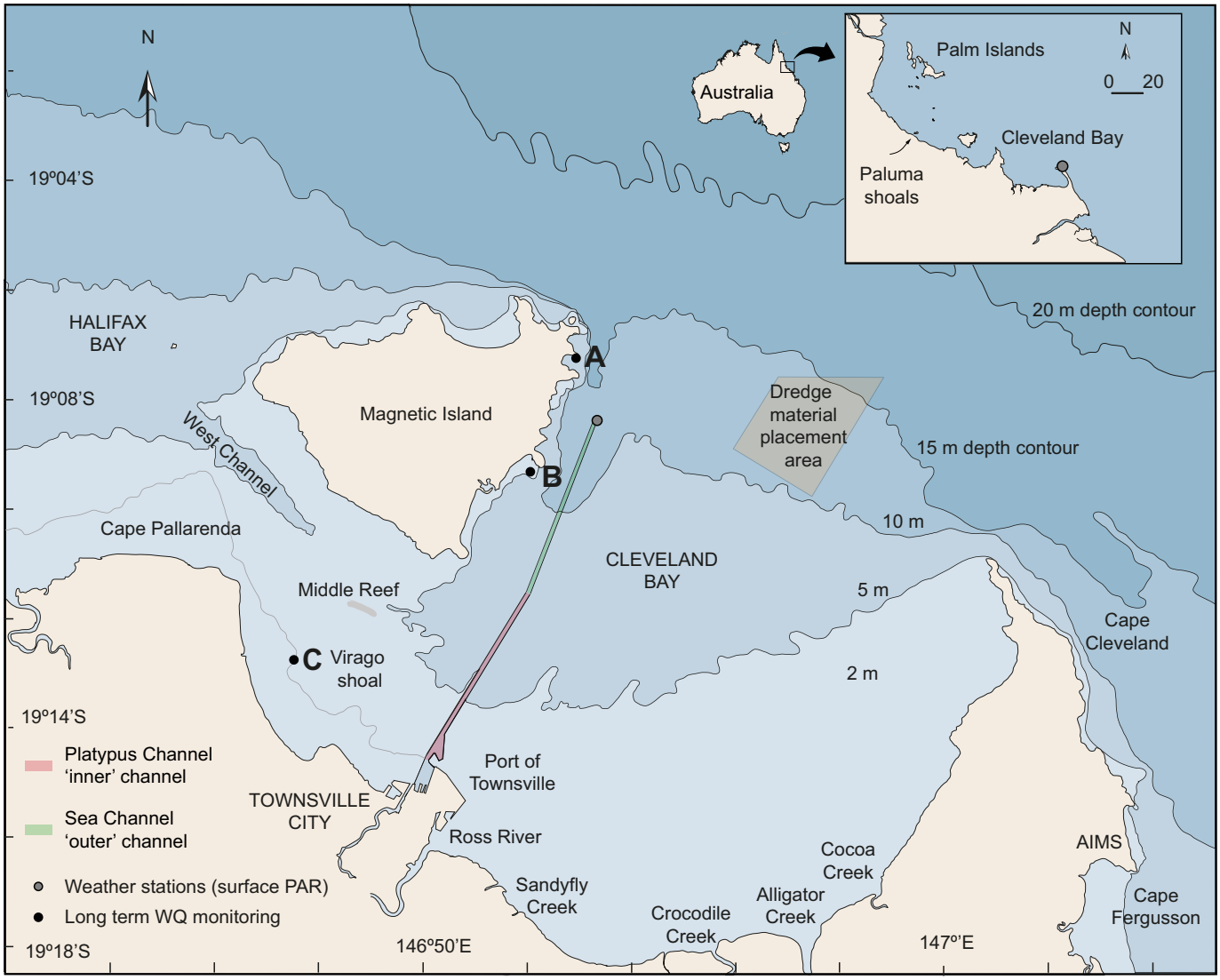


Fig. 1. Location map showing Cleveland Bay off the coastal city of Townsville, Australia in the inner central GBR showing sites at: (A) Florence Bay (−19.121722°, 146.883111°), depth 3.2 ± 2.1 m, (B) Geoffrey Bay (−19.155120°, 146.868340°), depth 4.0 ± 2.1 m, (C) Virago Shoal (−19.213180° 146.792370°), depth 3.9 ± 2.1 and the location of the coral and sponge collection sites near the Palm Islands (inset Figure). Surface measurements of PAR were obtained from the AIMS Automated Marine Weather and Oceanographic Station instruments in Cape Bowling Green (AIMS, 2020a) and Cleveland Bay (AIMS, 2020b) (see inset figure).

semidiurnal with a strong diurnal inequality and a ~4 m tidal range; however, tidal flows are believed to only have a minor influence on resuspension in the Bay (Anthony et al., 2004; Larcombe et al., 1995).

Annual or biannual maintenance dredging is needed of two connected shipping channels within the Bay (the Platypus and Sea Channel) to allow safe passage of ships to the mainland Port of Townsville (Fig. 1). Maintenance dredging occurs over about a 4–5 week period usually commencing in the second half of the year. The majority of the dredging is currently conducted by an 85 m long TSHD (trailing suction hopper dredge) with a 2900 m^3 capacity central hopper. Turbidity generation is associated with disturbance of the seabed by the drag head and by propeller wash, and sediment disposal at the ~3.7 × 3.7 km dredge material placement area (DMPA) in the centre of the Bay (Fig. 1).

2.2. In-situ turbidity and light time series

From September 2014 to August 2017, underwater measurements of turbidity and light were measured at 10-minute intervals at three sites within Cleveland Bay using submersible instruments mounted to a stainless-steel frame deployed at depths of 3–4 m. Turbidity was measured by optical scatter techniques using a WET Labs ECO-NTU sensor (WET labs, Philomath, Oregon, US) giving readings in Nephelometric Turbidity Units (NTU). Underwater light was measured as photosynthetically active radiation (PAR, 400–700 nm) using LI-COR Li-192 underwater quantum sensors (LI-COR, Nebraska, US, (see LI-COR Biosciences, 2018)). Each sensor had a cleaning mechanism to maintain the surface of the sensors free of biofouling and were retrieved for cleaning at approximately two-monthly intervals and replaced yearly with calibrated sensors.

Surface measurements of PAR were obtained from the Automated Marine Weather and Oceanographic Station at Cleveland Bay (AIMS, 2020b) and at Cape Bowling Green (AIMS, 2020a) (Fig. 1). All data were plotted and inspected for data anomalies and in some cases quarantined according to procedures described in Jones et al. (2015). Using the *gam* function from the *mgcv* package (Wood, 2006), Generalised Additive Models were fit individually for each site for each day using the available data. Daily light integrals (DLIs) were calculated as the sum of interpolated per second PAR values throughout the day from sunrise to sunset. DLI were calculated in a similar way for surface PAR obtained from the Cleveland Bay weather station (AIMS, 2020b). As data from this sensor were unavailable from the 29th of Nov 2015 to 9th Nov 2016, the surface light time series was filled in using data from the next nearest logger for which data were available which was Cape Bowling Green weather station (AIMS, 2020a) (Fig. 1 inset). Long-term time series of NTU and DLI were used to calculate running daily means across a range of time scales (1 h or 1 d through to 42 d) and were summarised as percentiles and cumulative probability plots (Jones et al., 2015).

2.3. Experimental setup and collections

Over a 28-day period corals and sponges were exposed to five different elevated SSCs and associated light reduction scenarios to generate a dose-response relationship using several sub-lethal physiological endpoints. The time frame was chosen as it encompasses the typical 2–4 week duration of the maintenance dredging projects in Queensland, Australia (Ports Australia, 2014), time frames of coral acclimation, as well as encompassing known natural periodicities in benthic irradiance in Cleveland Bay from clouds, turbidity and tides (Anthony et al., 2004).

The light reduction levels required to generate the dose-response relationship was guided by past experiments (Bessell-Browne et al., 2017a; Bessell-Browne et al., 2017b; Jones et al., 2020), the analysis of the long term underwater measurements of turbidity and light at the reef sites (see below), and a spectral solar irradiance model for Cleveland Bay (Jones et al., 2019b). The solar model is based on the Beer's law (Beer–Lambert–Bouguer law) and wavelength specific light attenuation coefficients determined from in-situ vertical profiling of turbid water with a free-falling hyper-spectral (5 nm increment) radiometer and simultaneous measurements of nephelometry-derived SSCs. The model allows estimates of the likely quantity of light and also the spectral profile of the underwater light field at a given water depth, SSC and sun elevation (zenith angle) (Jones et al., 2019b).

Five SSC treatment levels were chosen ranging from 2 to 15 mg L^{-1} (Table 1). Using the solar model the maximum (solar noon) irradiance levels (assuming no clouds), and the spectral shape of the light, was determined at depth of 5 m and solar elevation angle (from vertical) of 19° (Table 1). The depth was selected as it corresponds to the depth above which the majority of corals occur on the reefs of Magnetic Island (Ceccarelli et al., 2020), and the solar elevation angle chosen as it corresponds to the equinoxes and is most representative of an average of noon-time elevation angles over the year. From the model the maximum instantaneous PAR at solar noon (culmination) under the chosen SSC concentrations corresponded to a range of 210–2.2 μmol photons m^{-2} d^{-1} (Table 1). In the laboratory, corals and sponges were exposed to a 12-h light:dark cycle involving a sinusoidal ramping up from sunrise (06:00 h) until the noon maximum and ramping down to sunset (18:00 h) (light data for the first 7 days of the experiment is shown in Fig. 2A). This lighting regime resulted in DLIs that ranged over two orders of magnitude from ~6 to 0.06 mol photons m^{-2} d^{-1} (Table 1), which, based on past experiments (see above), was a light reduction range sufficient to generate a response over the 28-d experimental duration.

Suspended sediments change the spectral profile of underwater light, preferentially attenuating blue light (Fearns et al., 2019; Jones et al., 2016). The spectral shape (quality) of the light from the solar model (at solar noon) under a given SSC was also replicated in the experimental tanks using custom-made light fittings based on light-emitting diode (LED) technology and resulting in a peak irradiance of ~550 nm in the yellow-green range (Fig. 2B).

The laboratory experiment was conducted in 10 × 1200 L fibreglass tanks with 0.4 μm filtered flow-through seawater (FSW) in an environmentally controlled room within the National Sea Simulator (SeaSim) at the Australian Institute of Marine Science (AIMS), Townsville, Queensland (Fig. 1). Sediments used in the experiment were light brown in colour (Munsell colour 10YR6, RGB 124, 104, 53) and predominantly siliciclastic, collected from Middle Reef (−19.194278°, 146.813750°; Fig. 1). The sediments were screened to 2 mm and ground with a rod mill grinder to ~38 μm with a modal size of 25 μm measured using laser diffraction techniques (Mastersizer 2000, Malvern instruments Ltd., UK), resulting in predominately silt-sized sediment (Jones et al., 2016, Duckworth et al., 2017). Total organic content of the sediment was 0.25 ± 0.09% (*w*/w) analysed with a Shimadzu TOC-5000 carbon analyser (Shimadzu Corporation, Kyoto, Japan).

Table 1
Details of the experimental treatments employed. The values were derived from an empirical solar irradiance model and used to predict the light levels at a depth of 5 m and (at a zenith angle of 19° equivalent to the equinoxes). SSC = suspended sediment concentration, PAR = photosynthetically active radiation, DLI = daily light integral, and the ratio of blue (455 nm) to green (λ555 nm) light (see text).

Parameter	Units	Scenarios (treatments)				
		1	2	3	4	5
Nominal SSC	mg L^{-1}	2.5	5	7.5	10	15
Measured SSC		2.3 ± 0.2	5.1 ± 0.4	8.1 ± 0.4	10.5 ± 0.6	15.7 ± 0.8
MODEL (noon) PAR	μmol photons m^{-2} s^{-1}	227	82	31	12	2
PAR max (measured)		210	80	31	13	2
DLI (measured) (replicate tanks)	mol photons m^{-2} d^{-1}	5.78 5.83	2.19 2.19	0.85 0.85	0.36 0.36	0.06 0.06

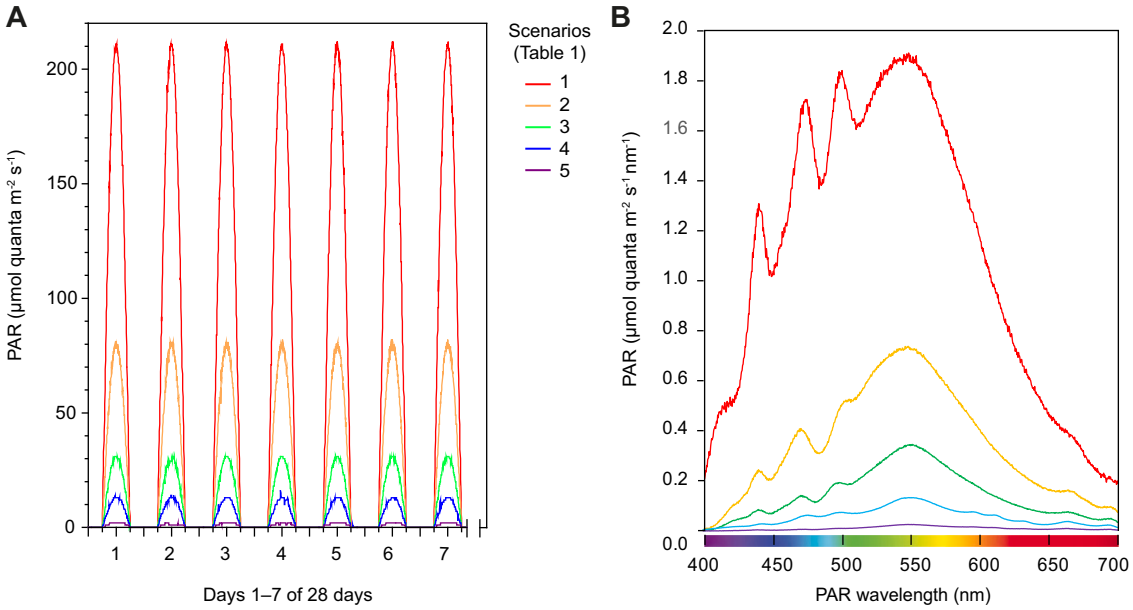


Fig. 2. A, B. (A) Measured instantaneous PAR levels in (µmol quanta m^{-2} s^{-1}) in the first 7 d of the 28-d experiments showing the 12 h L:D cycle in one of the replicate tanks per scenario. (B) Spectral profiles of the light in the different scenarios measured with a Jaz spectrometer (Ocean Optics Inc.) calibrated to a recently calibrated HL-2000 lamp, connected to a 5-m long 400-µm diameter fibre optic with a 3.9 mm diameter in-water cosine corrector attached (panel B).

The sediment dosing system and control mechanism has recently been described in Jones et al. (2020). Briefly, the system allows three complete turnovers of seawater per day per tank while maintaining SSCs at a constant level by episodic injection of a concentrated sediment slurry. Turbidity in each tank was measured using a Turbimax CUS31 nephelometer (Endress and Hauser, Germany) held in the turbidity sensing loop (Fig. 3), providing feedback to a programmable logic controller (PLC) system, which controlled sediment injection to the tanks via solenoids valves from a sediment delivery loop (Fig. 3). Water temperature was maintained at 25 ± 1.5 °C in all tanks over the course of the experiment, consistent with temperatures from the collection site. Various recirculating pumps were used to prevent any sediment deposition (Fig. 3).

Nephelometers were calibrated with Formazin and set to measure Formazin Nephelometric Units (FNU). Water samples were taken throughout the experiment ($n = 10$) to relate FNU to SSCs (mg L^{-1}) and the relationship determined by filtering water samples (250 mL) through pre-weighed 0.4 µm polycarbonate filters, which were then rinsed with deionised water, dried at 60 °C for 24 h and re-weighed (Table 1).

The lighting system used was different to the one described in Jones et al. (2020) and involved custom-made light fittings based on light-emitting diode (LED) technology that were capable of adjusting quantity and quality (spectral composition) of light above each tank. Each light was composed of 840 individual LEDs across 28 colours, assembled in four chips with a total power of 1.3 kW. The lighting system was fully integrated with the PLC system and each light was controlled by 19 independent channels. A High Output Light Sensors (HOPL) Quantum PAR sensor 2625 (Skye, UK, see LI-COR Biosciences (2018)) was positioned on the grid floor next to the specimens and connected to the PLC for feedback, allowing the PLC to control light intensity.

Two species of branching coral: *Acropora millepora* (Ehrenberg, 1834), *Pocillopora verrucosa* (Ellis & Solander, 1786), a foliose coral species, *Montipora aequituberculata* (Bernard, 1897) and a bioeroding sponge species, *Cliona orientalis* (Thiele, 1900) were collected from 5 m depth from the Palm Island group (Fig. 1). Fragments from five colonies of each of the coral species and two *C. orientalis* were collected using a mallet and chisel. Colonies were transported to the SeaSim at AIMS where partial colonies were fragmented into smaller clones (~5–10 cm length for corals and ~20–50 cm^2 surface area for sponges) and glued onto circular aragonite plugs for support. Clones were left to acclimate for six weeks in 1200 L holding tanks with flow-through seawater at 25 °C and 36 PSU salinity. Animals were fed daily using enriched *Artemia* spp. (targeted concentration in tanks of 0.5 nauplii mL^{-1}) and a mix of microscopic algae (2000 cells mL^{-1}). During the acclimation period, specimens were held under a 12-h light:dark cycle of linearly ascending (to a peak at noon) and then decreasing light levels and over the course of the day, resulting in a DLI of ~6 mol photons m^{-2} d^{-1}.

Each treatment consisted of two replicate tanks, resulting in a total of 10 individuals of each coral species ($n = 5$ per tank, with each genotype represented) and 8 individuals of *C. orientalis* per treatment. The experiment was ended after 28 days.

2.4. Survivorship, partial-mortality, and colour changes

All species were photographed on 0, 7, 14, 21 and 28 d using a high-resolution digital camera (Nikon D810) and assessed for mortality and partial mortality (i.e., tissue necrosis). Changes in colour were assessed using the software ImageJ (Version 1.52a) (Schneider et al., 2012) employing the histogram function to acquire mean pixel intensity on a black and white scale as previously described (Bessell-Browne et al., 2017a; Bessell-Browne et al., 2017b).

2.5. Symbiont density, pigments, and lipids

After the 28-d experimental period, samples were snap frozen in liquid nitrogen and stored at −80 °C until required for subsequent analyses. For symbiont density analysis, coral tissue was removed by air blasting in 30 mL of 0.5 µm FSW, with aliquots of the resulting blastate taken for symbiont density (1 mL, fixed in 10% buffered formalin), pigments (1 mL) and lipid (10 mL) analyses and the remaining skeleton wax dipped to determine surface area (Stimson and Kinzie, 1991). Symbiont density was determined by counting aliquots ($n = 6$) using a Neubauer haemocytometer containing 8 µL homogenised blastate, with a prior incubation in 1 M NaOH for 1 h required for digestion of *C. orientalis* tissue (Zamoum and Furla, 2012).

Pigments (Chl *a*) were obtained through a double extraction procedure using pre-chilled 95% ethanol (1 mL and 700 µL). During the first

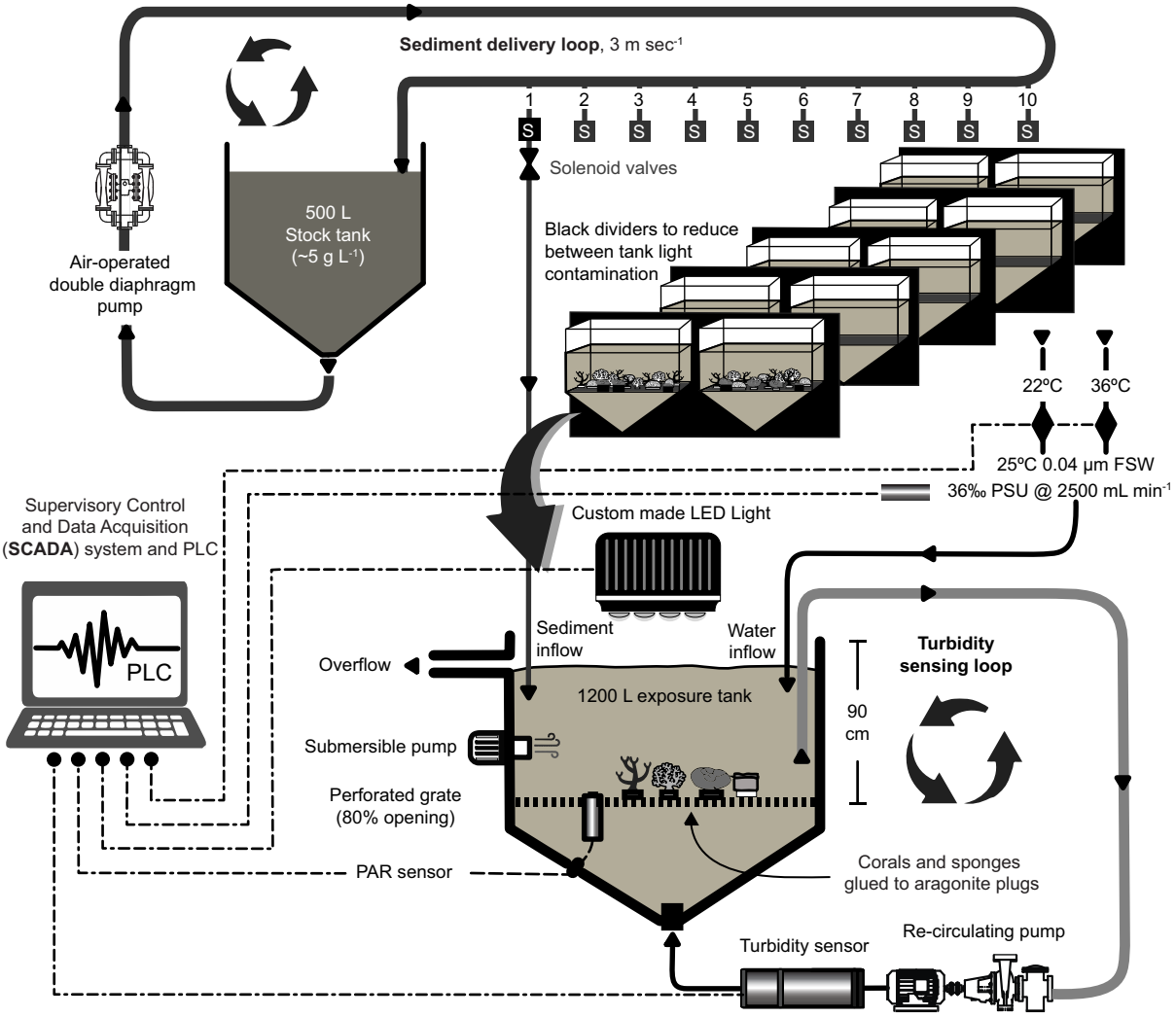


Fig. 3. Schematic diagram of the automated, computer-controlled sediment dosing system in SeaSim at AIMS, modified from Jones et al. (2020). Corals and sponges were held in 10 × 1200 L tanks receiving a continuous flow of filtered seawater with episodic injections of pulses of suspended sediments from a stock tank via a *sediment delivery* loop. SSC concentrations were monitored continuously in the *turbidity sensing* loop for each tank, providing feedback to the PLC system which maintained the SSCs at the desired levels. Light was provided by a custom-made LED lights above each tank which was also connected to the PLC which controlled spectral quality and quantity in each tank over a 12 h L:D cycle (see Fig. 2).

round of extraction, samples were sonicated on ice for 10 s at 40% amplitude, followed by centrifugation at 10,000 rpm for 5 min. The second round of extraction included a 30 min incubation on ice in the dark and 5 min centrifugation at 10,000 rpm. Extractions were combined and analysed on a Power Wave Microplate Scanning Spectrophotometer (BIO-TEK® Instruments, Inc., Vermont, USA) as previously described (Pineda et al., 2016) and standardised to estimate coral surface area (cm^2) or number of symbiont cells per replicate. Pigments from *C. orientalis* pinacoderm and mesohyl regions were similarly extracted and analysed following procedures described in Pineda et al. (2016) and standardised to sponge wet weight.

Total lipids and lipid classes were determined following the air-spraying method of Conlan et al. (2017). Freeze-dried samples were extracted using dichloromethane-methanol (2:1), filtered and washed with 4.5 mL of 0.44% KCl in methanol-H_2O (3:1). The bottom lipid layer was carefully recovered, dried-down under nitrogen and quantified. Lipid classes were determined using an Iatroscan MK-6 s thin layer chromatography flame ionisation detector (Mitsubishi Chemical Medience, Tokyo, Japan). Using silica gel S5-chromarods (5 µm particle size), samples (duplicates) were extracted following a two-step elution, with phosphatidylethanolamine (PE), phosphatidylserine and phosphatidylinositol (PS-PI), phosphatidylcholine (PC), and lysophosphatidylchloline (LPC) eluted first using dichloromethane: methanol: water (50:20:2) solvent system run to half-height (~15 min) and wax esters (WAX), triacylglycerol (TAG), free fatty acid (FFA), and sterol (ST) eluted next using n-hexane: diethyl ether: formic acid (60:15:1.5) solvent system run to full height (~30 min). In addition, 'acetone mobile polar lipids' (AMPL) were also quantified using the 1-monopalmitoyl glycerol standard (Sigma-Aldrich Co., USA), since glycolipids commonly elute with monoacylglycerols and pigments (Parrish et al., 1996). Storage lipid (WAX, TAG and FFA) to structural lipids (PE, PS-PI, PC, LPC, ST, AMPL) ratios were computed for each coral or sponge.

2.6. Statistical analyses

Treatment effects were examined using Generalised Linear Mixed Models (GLMMs) using the Gamma family with a log-link function, with tank as a random factor. If appropriate, multiple comparisons were undertaken using the Dunnett's test to identify significant differences from the control (e.g. 5.7 DLI and 2.5 mg L^{-1}). Analyses were carried out in *R* (v 3.6.3) using the *glmer* function of the *lme4* package (Bates et al., 2015) and the *glht* function of the *multcomp* package (Hothorn et al., 2008). PERMANOVA, using 9999 permutations, was used to identify

differences in the lipid classes between treatments. If pairwise comparisons resulted in insufficient unique permutations, Monte-Carlo-derived *p*-values were used. Multivariate analyses were carried out using PRIMER 6/PERMANOVA+ v1.0.2 (Plymouth, UK). Response thresholds were derived for all species and variables that showed a strong consistent change as a function of decreasing light levels. The estimation of No Effect Concentrations (NEC), and 10 and 50% effect concentrations (EC10 and EC50) were calculated in *R* using the function *fit.jagsMANEC* in the package *jagsNEC* (Fisher et al., 2020). The function *fit.jagsMANEC* fits a set of commonly used dose-response models and threshold models adapted from (Fox, 2010), and returns a model-weighted estimate of predicted posterior values, based on deviance information criteria (DIC) model weights. In all cases, mixing of MCMC chains were assessed visually, and where models showed poor mixing, even with a relatively large burn-in, these were excluded from model averaged estimates of endpoints. Only *P. verrucosa* showed sufficient declines across the physiological variables for thresholds to be estimated, although concentration-response relationships were able to be fit

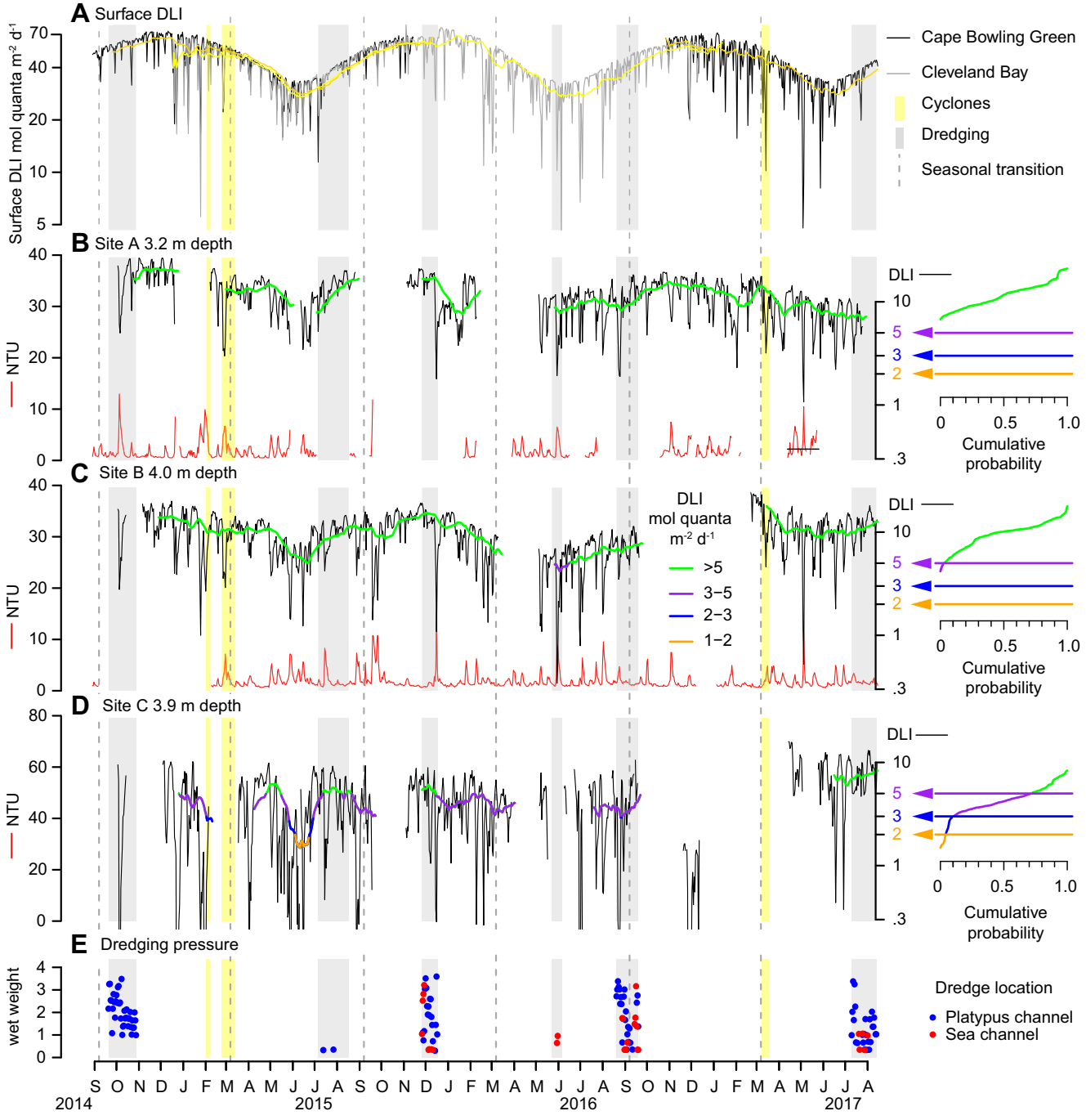


Fig. 4. Time series plots showing (A) surface PAR and (B, C, D) underwater PAR (as DLIs, mol photons m^{-2} d^{-1}) and turbidity as nephelometric turbidity units (NTU) measured at the three long-term water quality monitoring sites (Fig. 1). Grey vertical bars represent periods of annual maintenance dredging with (E) the amount of dredging indicated as wet weight ($\times 10^3$ kg) removed per day. Coloured lines through the light data represent the 28-d running mean and different colours represent periods when the running mean is below the given DLI (as shown in the legend in C). The right-hand side plots show cumulative probability profiles for the 28-d running mean DLIs for each site. The same colour coding system is used representing the proportion of observations above and below the given DLI range. (For interpretation of the references to colour in this figure legend, the reader is referred to the web version of this article.)

to the storage/structural lipid ratios for all species.

3. Results

3.1. Turbidity and light time series

Surface (above water) light levels exhibited the expected cyclical seasonal pattern with the 28-d running mean ranging from 50 to 60 mol photons m^2 d^{-1} in the summer to 30–35 mol photons m^2 d^{-1} in the winter (Fig. 4A). The heavy cloud cover associated with cyclones Marcia (15–26 February 2015), Nathan (9–25 March 2015) and Debbie (23–30 March 2017) influenced the light availability; however, over the study period there were frequent periods of low light in both winter and summer caused simply by high cloud cover unrelated to notable meteorological events (Fig. 4A).

Maximum instantaneous underwater PAR levels (measured every 10 mins) were 1342 and 1254 μmol photons m^{-2} s^{-1} at the two more seaward sites (sites A and B respectively) and 917 μmol photons m^{-2} s^{-1} at the inner most reef site (site C). Mean (yearly) DLIs were 12.0 and 10.0 mol photons m^{-2} d^{-1} at sites A and B respectively, which were 2.6–2.2 × more than at site C (~4.6 mol photons m^{-2} d^{-1}) (Fig. 4).

Maximum NTU values (from the 10 min readings) ranged from a minimum of <0.5 across all sites to 33.1, 60.7 and 115.5 NTU at sites A, B and C, respectively. Over the study mean daily NTU values were ~1.9 NTU at the more seaward reef sites facing the open ocean reef (sites A and B) and ~3.6 × lower than at site C (~6.9 NTU) (Fig. 4).

Analyses of operational data from the Port of Townsville showed that over the 3-year water quality monitoring period there were four separate occasions when the trailing hopper suction dredge (TSHD) was operating in the Sea Channel totalling 29 days (Fig. 4E). Of those days, the TSHD was actively dredging for 114 h, and 306,703 t (wet sediment) was removed from the seabed and taken to the dredge material placement area.

The underwater running mean DLI values, cumulative probability plots and coincidence of low light periods shown in Fig. 4 are discussed further below (see *Risk assessing dredging*).

Fig. 5 shows a running means/percentiles analysis using the yearly light and turbidity data from Site B (Fig. 1), showing different percentile values of different running mean periods from 1 to 42 d for light and 1 h–42 d (i.e., 6 weeks for NTU) (see Fisher et al. (2015); Jones et al. (2016); Jones et al. (2015) for further details). To avoid biased averages, no running mean value was calculated if more than 20% of the data points for any running mean time-period were missing. Once calculated, the percentile (*P*) values of the different running mean values were plotted on the y-axis against the running mean time-period on the x axis, generating a series of curves (Fig. 5).

The analysis shows that over 1 day the P_{100} DLI at Site B was 24.1 mol photons m^{-2} i.e., the day with the most underwater light recorded at Site B over the three-year study (Fig. 5A). Over successively longer running mean intervals (7, 14, 21, 28 days etc.) the upper percentile values ($P_{100,\ 99,\ 95}$ etc) progressively decreases, as benthic light availability will typically decrease (from turbidity and clouds) from the best-case scenario. For the lower percentiles ($P_{0,\ 5}$ etc) the situation is similar but in the opposite direction: the lowest DLI value was <0.2 mol photons m^{-2} (functionally equivalent to a day in darkness), but as the running mean period increases the DLI values increase – as conditions will ultimately improve from a worst case scenario (Fig. 5A). Further, summary statistics for all the long-term water quality monitoring sites showing the percentile values of the daily light integral or turbidity for the running mean periods up to 42 d for all sites can be found in Table 2.

For NTUs, the analysis in Fig. 5B shows that periods of very high (tens of) NTUs are relatively short-term phenomena. The P_{100} for the shortest running mean period (1 h) was 44 NTU and 3× more than a 1-day running mean P_{100} and 5× more than the 7-d running mean scenario.

For light, the lower percentile values are of most interest as they could represent possible light limitation. Although the worst DLI value was <0.3 mol photons m^{-2} d^{-1}, over running mean periods greater than 10 days the worst case (P_{100}) DLI values gradually increased to >3 mol photons m^{-2} (see further below under *Risk assessing dredging*).

3.2. Laboratory-based exposure study

All corals and sponge species survived the 28-d experiment with no mortality or partial mortality. Colour changes occurred over the course of the experiment with *P. verrucosa* showing the most marked changes, with clear lightening of the tissues observed by day 14 in the 0.85, 0.34 and 0.06 mol photons m^{-2} d^{-1} treatments (Fig. 6A). By day 28 *P. verrucosa* were 52% paler in the lowest light treatment than those in the 5.7 and 2.2 mol photons m^{-2} d^{-1} treatments, with a significant difference between the control and two lowest light treatments observed (Table 3). While *M. aequituberculata* also displayed colour changes over the course of the experiment, individuals from the 5.7 mol photons m^{-2} d^{-1} treatment were paler than those at 0.06 mol photons m^{-2} d^{-1} by day 28 (Fig. 6A). *C. orientalis* from the two highest light treatments showed a slight darkening after day 7 but had lightened by the end of the experimental period, with all five light/SSC treatments lightened by the end of the experiment (Fig. 6A).

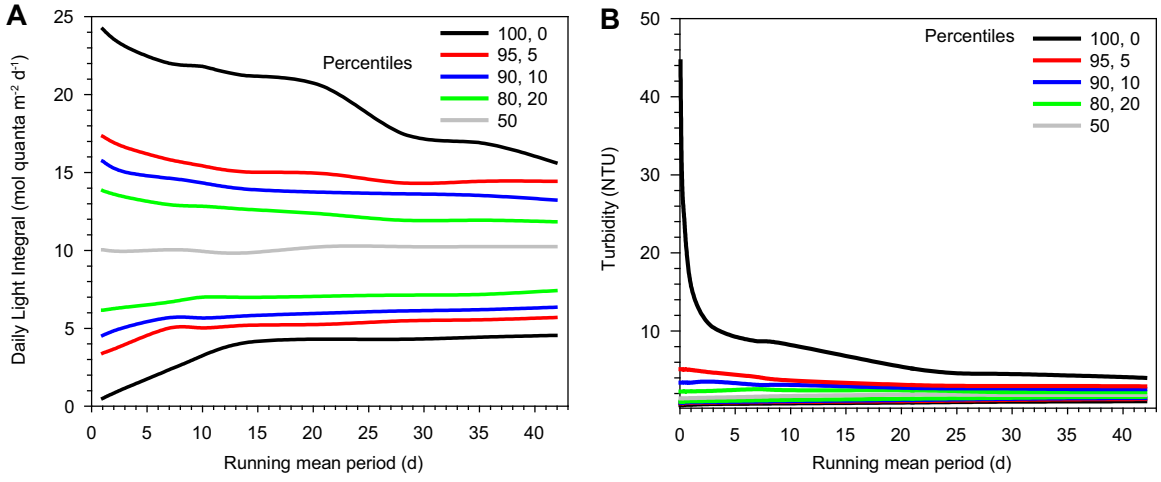


Fig. 5. (A, B) Site B (Geoffrey Bay) Running mean percentiles analysis showing the P_{100} to P_0 daily light integral (mol photons m^{-2} d^{-1}) over running mean periods from 1 to 42 d for light or 1 h–42 d for turbidity. Site B was chosen as the representative site for the analysis as it is the nearest coral reef to the Sea Channel and most likely to be influenced by dredging activities.

Table 2
Light and turbidity summary statistics for the three long-term water quality monitoring sites (A = Florence Bay, B = Geoffrey Bay and C = Virago Shoal, see Fig. 1) showing the percentile (P) values of the daily light integral (DLI, mol photons m^2) and turbidity (NTU) for the running mean periods of 1, 3, 7, 10, 14, 21, 28, 35 and 42 days. For turbidity, *P* values were also calculated for running mean periods of 1, 6 and 12 h. The 3-point colour scale is red for the lowest (DLI) or highest (NTU) value, green for the highest (DLI) or lowest (NTU) and yellow for the 50th percentile with all other values coloured proportionally.

		Daily light integral (mol photons m^2)									Turbidity (NTU)								
	d	0th	5th	10th	20th	50th	80th	90th	95th	100th	0th	5th	10th	20th	50th	80th	90th	95th	100th
A	1 h	–	–	–	–	–	–	–	–	–	0.5	0.5	0.5	0.6	1.1	2.6	4.1	5.6	29.9
	6 h	–	–	–	–	–	–	–	–	–	0.5	0.5	0.6	0.7	1.1	2.5	4.0	5.5	23.8
	12 h	–	–	–	–	–	–	–	–	–	0.5	0.5	0.6	0.7	1.2	2.4	3.9	5.2	17.2
	1 d	1.1	4.1	5.3	7.4	11.6	16.2	18.7	20.4	26.6	0.5	0.5	0.6	0.7	1.2	2.3	3.6	4.9	13.1
	3 d	2	4.8	6	8	11.5	16	18	20	26.3	0.5	0.6	0.6	0.8	1.3	2.3	3.5	4.7	9.7
	7 d	4.3	5.9	6.8	8.1	11.5	15.6	17.9	19.9	24	0.5	0.7	0.7	0.9	1.4	2.1	3.0	4.2	6.9
	10 d	5.4	6.5	7	8.3	11.6	15.4	17.6	19.9	23	0.6	0.7	0.8	1.1	1.4	2.1	3.2	3.9	6.5
	14 d	5.8	7	7.4	8.3	11.5	15.3	17.1	20	22.3	0.6	0.8	1.0	1.1	1.5	2.3	3.0	3.7	5.7
	21d	6.4	7.4	7.8	8.5	11.6	14.7	16.8	20.1	21.8	0.6	0.9	1.0	1.1	1.6	2.3	2.8	3.1	4.3
	28 d	6.7	7.5	7.9	8.8	11.7	14.3	16.6	20.2	21	0.8	0.9	1.0	1.2	1.7	2.3	2.5	3.3	3.5
	35 d	6.7	7.5	8.1	9	11.4	14.3	16.4	20.1	21.3	0.9	1.0	1.0	1.2	1.7	2.2	2.9	3.0	3.3
	42 d	6.9	7.5	8.3	9.1	11.3	14.1	15.7	19.9	21	0.9	1.0	1.0	1.3	1.8	2.1	2.7	2.8	3.3
B	1 h	–	–	–	–	–	–	–	–	–	0.5	0.7	0.8	0.9	1.4	2.3	3.4	5.1	44.5
	6 h	–	–	–	–	–	–	–	–	–	0.5	0.7	0.8	1.0	1.4	2.2	3.4	5.1	27.1
	12 h	–	–	–	–	–	–	–	–	–	0.5	0.8	0.9	1.0	1.4	2.3	3.4	5.1	21.6
	1 d	0.3	3.2	4.4	6	9.9	13.7	15.6	17.2	24.1	0.6	0.8	0.9	1.0	1.4	2.3	3.4	5.0	15.7
	3 d	1	3.8	4.9	6.2	9.8	13.3	14.9	16.5	23	0.6	0.8	0.9	1.0	1.5	2.3	3.5	4.7	10.5
	7 d	2.2	4.9	5.5	6.5	9.9	12.8	14.5	15.7	21.9	0.7	0.9	1.0	1.1	1.6	2.6	3.1	4.1	8.7
	10 d	3.1	4.9	5.5	6.8	9.8	12.7	14.2	15.3	21.7	0.7	0.9	1.0	1.2	1.7	2.4	3.1	3.7	8.2
	14 d	3.9	5	5.7	6.8	9.7	12.5	13.8	14.9	21.1	0.8	0.9	1.1	1.2	1.8	2.4	3.0	3.2	6.5
	21d	4.1	5.1	5.8	6.9	10.1	12.2	13.6	14.8	20.4	0.8	1.0	1.2	1.3	1.9	2.4	2.7	3.1	5.2
	28 d	4.2	5.3	6	7.1	10.1	11.9	13.5	14.1	17.8	0.9	1.1	1.3	1.4	1.8	2.2	2.7	3.0	4.5
	35 d	4.3	5.4	6	7	10.1	11.8	13.4	14.3	16.8	1.0	1.2	1.4	1.5	1.8	2.2	2.6	3.0	4.3
	42 d	4.4	5.5	6.2	7.3	10.1	11.7	13.1	14.3	15.5	1.0	1.3	1.4	1.6	1.8	2.2	2.5	2.9	4.0
C	1 h	–	–	–	–	–	–	–	–	–	0.5	1.2	1.4	1.8	3.4	11.5	18.1	24.1	97.1
	6 h	–	–	–	–	–	–	–	–	–	0.5	1.3	1.5	1.9	3.7	12.3	18.4	24.8	67.0
	12 h	–	–	–	–	–	–	–	–	–	0.5	1.3	1.5	2.0	4.0	13.2	18.9	25.3	65.9
	1 d	0.0	0.3	0.6	1.7	4.3	7.2	8.8	10.2	15.9	0.5	1.4	1.6	2.1	4.9	14.4	19.7	25.7	52.0
	3 d	0.1	0.5	1.1	2.1	4.3	6.8	8.1	9.6	15.1	1.0	1.5	1.8	2.4	5.8	15.0	19.8	24.0	35.4
	7 d	0.2	0.9	1.6	2.5	4.4	6.6	7.8	8.8	15.1	1.2	1.8	2.1	2.9	6.9	13.4	17.6	20.6	32.0
	10 d	0.4	1.1	1.7	2.7	4.3	6.4	7.4	8.6	13.2	1.2	1.9	2.2	3.3	7.0	13.1	15.9	19.0	31.0
	14 d	0.5	1.4	2.1	2.9	4.4	6.2	7.4	8.5	10.9	1.3	2.2	2.6	3.5	7.4	12.4	15.0	18.5	25.4
	21d	0.7	1.6	2.7	3.2	4.2	5.9	7.0	8.0	10.3	1.8	2.8	3.4	4.7	7.8	12.3	14.7	17.6	20.9
	28 d	1.5	2.2	3.0	3.4	4.2	5.5	6.8	7.4	8.3	2.3	4.0	4.5	5.9	7.9	12.5	15.2	16.8	17.5
	35 d	1.6	2.2	3.1	3.5	4.2	5.3	6.8	7.3	8.2	4.0	4.7	5.2	5.8	9.3	13.1	14.7	15.2	16.7
	42 d	1.7	2.5	3.2	3.5	4.3	5.1	6.8	7.3	8.2	4.7	5.0	5.4	6.3	9.6	13.0	14.1	15.3	16.2

There were also significant differences in the densities of algal symbionts identified between the treatments for all coral species (Fig. 6B). Symbiont densities were highest at 0.85 mol photons m^{-2} d^{-1} and significantly different from the control for *A. millepora* and *M. aequituberculata* (Table 3). In contrast, *P. verrucosa* symbiont densities decreased rapidly between the highest light treatments and 0.85, 0.34 and 0.06 mol photons m^{-2} d^{-1} (Fig. 6B, Table 3). While symbiont densities in *P. verrucosa* decreased rapidly at light levels of 0.85 mol photons m^{-2} d^{-1}, the amount of Chl *a* per cell showed an opposite pattern with the highest concentrations observed at 0.85 and 0.34 mol photons m^{-2} d^{-1} (Fig. 6B). *A. millepora* symbiont Chl *a* levels were lowest at 0.85 mol photons m^{-2} d^{-1}, whereas *M. aequituberculata* symbiont pigment levels were lowest in the highest light treatment (Fig. 6B). Symbiont density in *C. orientalis* was greatest in the two lowest light treatments; however, no significant differences were identified (Fig. 6B, Table 3).

Significant differences in tissue pigment concentrations were also identified between light/SSC treatments for all species (Fig. 6C). *A.*

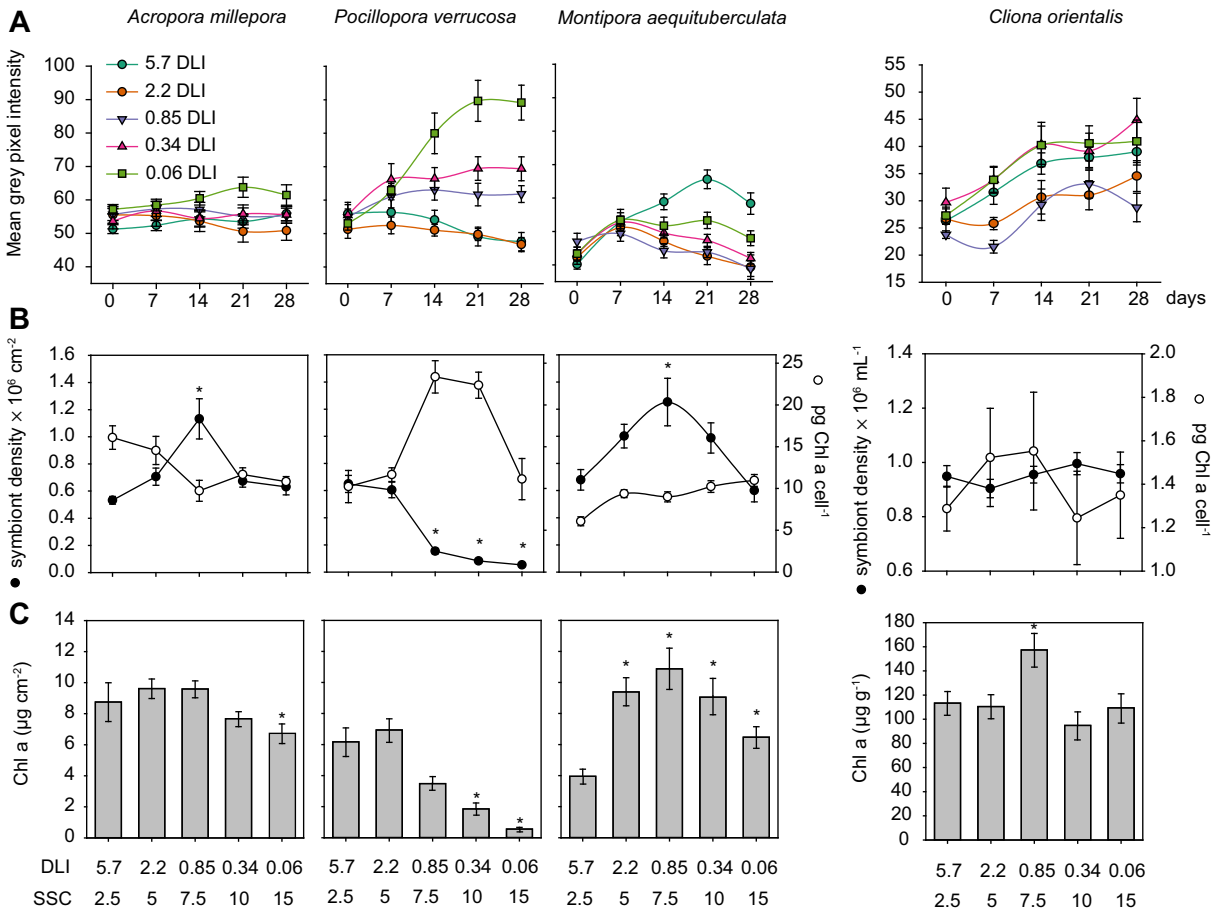


Fig. 6. (A) Mean grey pixel intensity for each of the species exposed to five turbidity treatments over the course of the 28-d experiment. The higher the pixel value, the brighter/lighter the coral or sponge. (B) Symbiotic dinoflagellate density ($\times 10^6$ cm^{-2}) for each of the species (black) and concentration of Chl *a* in symbiont cells (white). (C) Concentration of total Chl *a* (µg cm^{-2} for corals and µg g^{-1} for *C. orientalis*). For all panels, note the different units and scale for *C. orientalis*. Error bars represent 1 S.E. and * denotes a significant difference from the control (e.g. 5.7 DLI/2.5 SSC) according to Dunnett's multiple comparison test.

Table 3
Summary of the *p*-values from the Dunnett's multiple comparison test, using a daily light integral (DLI, mol quanta m^{-2} d^{-1}) of 5.7 as the control, for each of the species and response variables tested. For individual lipid classes, p(MC)-values from PRIMER/PERMANOVA+ pairwise tests are listed. Significant p-values (<0.05) are bolded.

	DLI	Colour changes	Symbiont density	Chl a conc	Total lipids	Lipid ratio	Lipid classes
Acropora millepora	2.2	0.324	0.564	0.784	**<0.001**	**<0.001**	**0.003**
(coral)	0.85	0.999	**0.013**	0.799	**<0.001**	**<0.001**	**0.009**
	0.34	1.000	0.702	0.536	0.820	**<0.001**	**0.024**
	0.06	0.319	0.876	**0.048**	0.999	**0.002**	**0.004**
Pocillopora verrucosa	2.2	0.999	0.982	0.992	**<0.001**	**<0.001**	**0.004**
(coral)	0.85	0.098	**<0.001**	0.061	**<0.001**	**<0.001**	**0.003**
	0.34	**0.006**	**<0.001**	**<0.001**	**<0.001**	**<0.001**	**0.008**
	0.06	**<0.001**	**<0.001**	**<0.001**	**<0.001**	**<0.001**	**0.001**
Montipora aequituberculata	2.2	**<0.001**	0.246	**<0.001**	0.994	0.104	0.356
(coral)	0.85	**<0.001**	**0.038**	**<0.001**	0.942	0.177	0.316
	0.34	**0.004**	0.524	**<0.001**	0.955	0.143	0.324
	0.06	0.150	0.984	**0.050**	0.744	**0.021**	0.265
Cliona orientalis	2.2	0.659	0.725	0.999	0.802	**0.040**	0.130
(sponge)	0.85	**0.026**	1.000	**0.040**	0.946	**<0.001**	**0.023**
	0.34	0.549	0.726	0.456	0.933	**<0.001**	**0.015**
	0.06	0.981	0.999	1.000	0.386	**<0.001**	**0.035**

millepora Chl *a* concentrations in the lowest light treatment were significantly lower than the control (e.g. 5.7 mol photons m^{-2} d^{-1}) (Table 3). Again, the most noticeable differences between treatments were observed for *P. verrucosa*, with significantly lower pigment levels at 0.34 and 0.06 mol photons m^{-2} d^{-1} compared to 5.7 mol photons m^{-2} d^{-1} (Fig. 6C, Table 3). Pigment concentrations in *M. aequituberculata* mirrored trends observed in symbiont densities, with Chl *a* highest at 0.85 mol photons m^{-2} d^{-1} (Fig. 6C) and each treatment being significantly different from the control (Table 3). Similarly, Chl *a* levels were highest and significantly different from the control at 0.84 mol photons m^{-2} d^{-1} in *C. orientalis* (Fig. 6C).

The percentage of total lipids varied between species and the five

light/SSC treatments (Fig. 7A). For *A. millepora* the amount of total lipids significantly decreased between 5.7 and 2.2 mol photons m^{-2} d^{-1} (Table 3), but increased again at the two lowest light treatments, whereas little changes were observed between the light/SSC treatments for *M. aequituberculata* (Fig. 7A). However, both species displayed a decrease in the ratio of storage to structural lipids at light levels lower than 5.7 mol photons m^{-2} d^{-1}. Similarly, the ratio of storage to structural lipids steadily declined as light levels decreased for *P. verrucosa*; however, unlike the other species, this decline was mirrored by a significant reduction in the percentage of total lipids (Fig. 7A, Table 3). While *C. orientalis* displayed a similar pattern to the corals with the ratio of storage to structural lipids, the percentage of total lipids increased at 2.2 mol photons m^{-2} d^{-1} followed by a decrease as light declined (Fig. 7A). Nine different lipid classes, encompassing both storage and structural lipids, were identified in the corals and *C. orientalis* from the different light/SSC treatments (Fig. 7B). A significant difference in the structure of lipid classes was identified in *A. millepora* and *P. verrucosa* between the control (5.7 mol photons m^{-2} d^{-1}) and all other treatments (Table 3). This is not surprising given the clear decrease in the ratio of storage to structural lipids from 5.7 to 2.2 mol photons m^{-2} d^{-1} predominantly driven by a decrease in TAG and to a lesser extent WAX. Differences between the lipid classes were also observed in *C. orientalis* between the control and 0.85, 0.34 and 0.06 mol photons m^{-2} d^{-1} (Table 3). As with the corals, there was a decrease in the ratio of storage to structural lipids in *C. orientalis*, with sponges exposed to control light/SSC levels having a higher percentage of TAG than those in the higher SSC treatments (Fig. 7B).

Since all the species in the experiment displayed a consistent response with decreasing light with respect to the ratio of storage to structural lipids, thresholds were derived for the point at which this transition occurs, with EC50 values estimated from the model averaged predicted values. The estimated EC50s varied between species but were most similar for *A. millepora* and *P. verrucosa* (Fig. 7C) at 4.0 and 3.4 mol photons m^{-2} d^{-1} respectively. *M. aequituberculata* had the lowest estimated EC50 for the corals at 1.5 mol photons m^{-2} d^{-1} (Fig. 7C). The estimated EC50 for *C. orientalis* was higher than *M. aequituberculata* at 1.9 mol photons m^{-2} d^{-1} (Fig. 7C) but lower than the two other coral species.

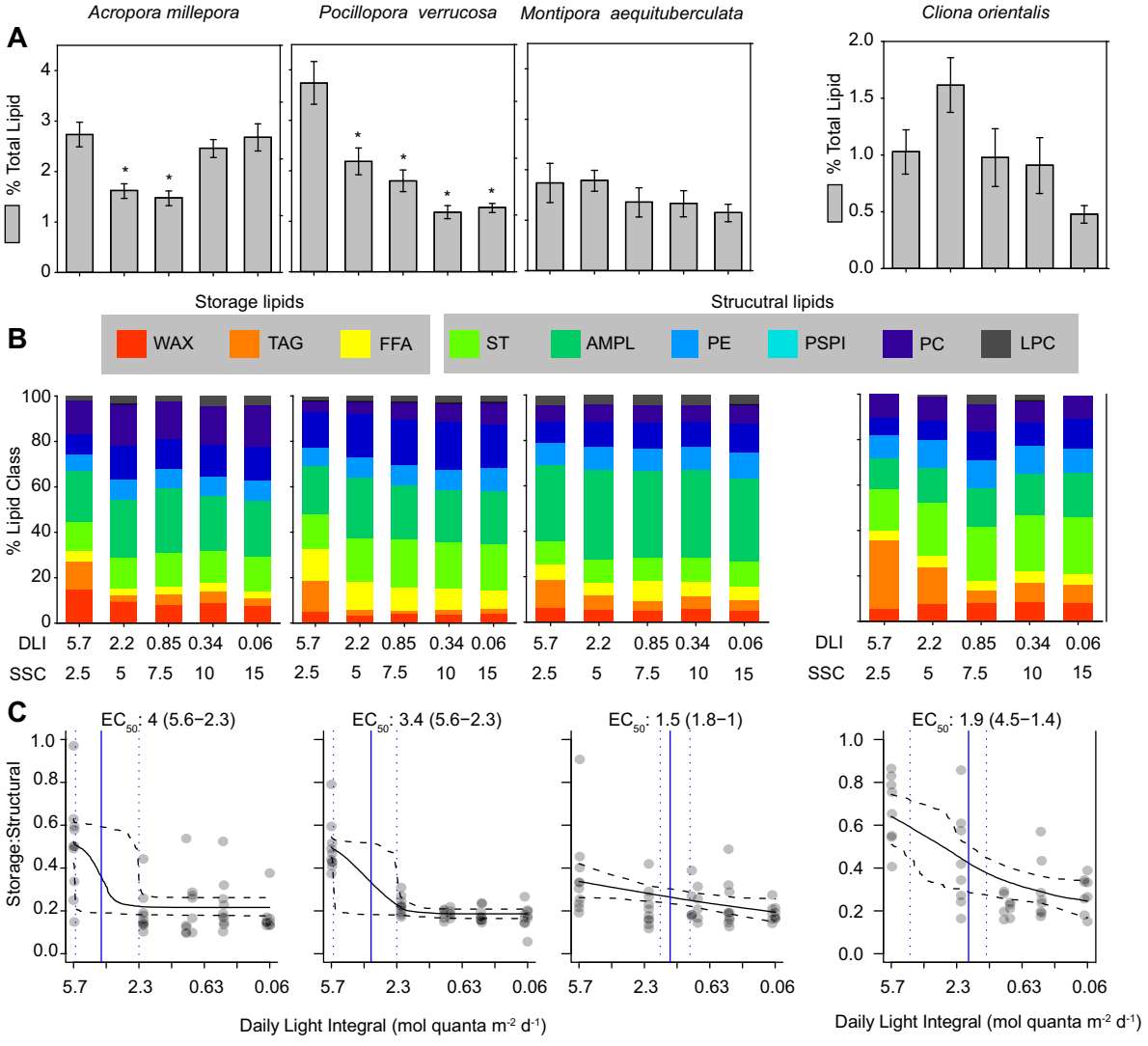


Fig. 7. (A) Percent total lipids for each of the species. Note the different scale for *C. orientalis*. Error bars represent 1 S.E and * denotes a significant difference in total lipids from the control (e.g. 5.7 DLI) according to Dunnett's multiple comparison test. (B) Lipid classes for each of the species under the five turbidity treatments where WAX = wax esters, TAG = triacylglycerol. FFA = free fatty acid, ST = sterol, AMPL = acetone mobile polar lipids, PE = phosphatidylethanolamine, PS-PI = phosphatidylserine and phosphatidylinositol, PC = phosphatidylcholine, LPC = lysophosphatidylchloline. (C) Concentration–response functions for all four species based on rescaled (0–1) ratio of storage to structural lipids. The black solid line shows the fitted model and the solid, vertical blue line the derived relative EC50 threshold values, with 95% credible intervals for both the model and the EC50 indicated by dashed lines. Models fitted using the *jagsNEC* package in *R*, see Methods. (For interpretation of the references to colour in this figure legend, the reader is referred to the web version of this article.)

In addition to the consistent response of decreasing lipid ratios with light stress, *P. verrucosa* also displayed similar responses with respect to symbiont density, total Chl *a* concentrations and colour/bleaching. Therefore, thresholds were also derived for these response variables, which included NEC and estimated EC10 and EC50 values. For this suite of response variables both the NEC and EC10 thresholds were lower than the EC50 value observed for the lipid ratio for this species (Fig. 8). For instance, the 10% loss of algal symbionts threshold was 2.71 mol photons m^{-2} d^{-1} and the 10% decrease in total Chl *a* was 1.68 mol photons m^{-2} d^{-1} (Table 4).

Table 4
Model averaged DLI (mol photons m^{-2} d^{-1}) threshold values for *P. verrucosa* which correspond to the red, orange, and blue vertical lines of Fig. 8.

	Symbiont density	Chl *a*	Colour intensity
NEC	2.74 (3.63–2.14)	1.52 (2.39–1.05)	2.04 (3.30–1.32)
EC10	2.71 (3.83–1.65)	1.68 (3.93–1.04)	1.9 (3.58–1.13)
EC50	1.48 (1.94–1.18)	0.88 (1.43–0.54)	0.63 (1.04–0.35)

4. Discussion

Elevated suspended sediment concentration and the associated turbidity (water cloudiness) is widely cited as a hazard associated with dredging and a pressure for coastal and terrestrially influenced nearshore environments of the inner central Great Barrier Reef (GBR) Marine Park. One of the key cause-effect pathways is light attenuation and a reduction in underwater light availability for benthic photoautotrophs (Jones et al., 2016). The three-year dataset collected using LI-COR (Nebraska, US) sensors in the current study is the longest to date of benthic light within the turbid-zone inshore communities of the GBR. There are remarkably few published studies where light levels have been quantified in the coastal reefs of the GBR – see for example Anthony and Connolly (2004); Cooper et al. (2008); Cooper et al. (2007); Jones (2008); Whinney et al. (2017). All these studies used low cost, commercially available or self-assembled instruments that were *user calibrated* against other light sensors, typically LI-COR sensors. The manufacturer-recommended calibration procedure has been questioned in some instruments (Dunne, 2010; Shaffer and Beaulieu, 2012), and their suitability for use in measuring absolute rather than relative light levels in marine environmental monitoring has also been questioned (Shaffer and Beaulieu, 2012). The spectral and cosine responses of the sensors have not been not described (Dunne, 2010) and it is not clear if the sensors have ultraviolet and infrared cut off filters and are measuring only in the 400–700 nm PAR range. Light-based above and below water monitoring programs using fit-for-purpose instruments seems a necessity to further understand the risk of enhanced sediment run-off to the inshore turbid water communities.

4.1. Turbidity patterns and light time series

The coral zonation pattern in the turbid-zone inshore communities is highly compressed or truncated in these *shallow water mesophotic* environments (Morgan et al., 2016), and at the study site the majority of corals, especially branching species, occur in less than 5 m of water (Ceccarelli et al., 2020). In the current study, daily light integrals measured at 3–4 m depth (with a ± 2 m tidal range) on the reefs around Magnetic Island (~19°S) ranged from 0.2–27 mol photons m^{-2} $day^{-1}$and averaged ~10–12 mol photons m^{-2} day^{-1} over the study. Average underwater values were 30% higher in summer than in winter (which were defined by the timing of the solstices) reflecting seasonal changes in solar elevation angles and day lengths. Low light, caliginous, periods occurred more frequently in the winter; however, summertime low light periods also occurred. These were typically associated with cyclones or more commonly monsoonal troughs that can bring very heavy cloud cover with associated high intensity rainfall events. The occassionally high turbidity levels measured over this study indicated why it is called the turbid-zone, and turbidity levels were in line with results from previous studies for Cleveland Bay (Larcombe et al., 1995; Macdonald et al., 2013; Orpin et al., 2004). The main characteristic was the strong temporal variability, which is well known for such water quality datasets in coastal environments, influenced by a range of factors such as waves, currents and bed type (Larcombe et al., 1995; Storlazzi and Jaffe, 2008; Storlazzi et al., 2004; Verspecht and Pattiaratchi, 2010).

This variability in turbidity, or benthic light availability, can be characterised using exceedance curves to describe a site based on the proportion of days that turbidity (as NTUs) or light (as DLIs) are below or above a given value – for example turbidity values may exceed 40 NTU for 40 days per year (see Larcombe et al., 2001). However, from a physiological perspective, what is far more important to know is when the exceedances occur in time i.e., consecutively, or intermittently and

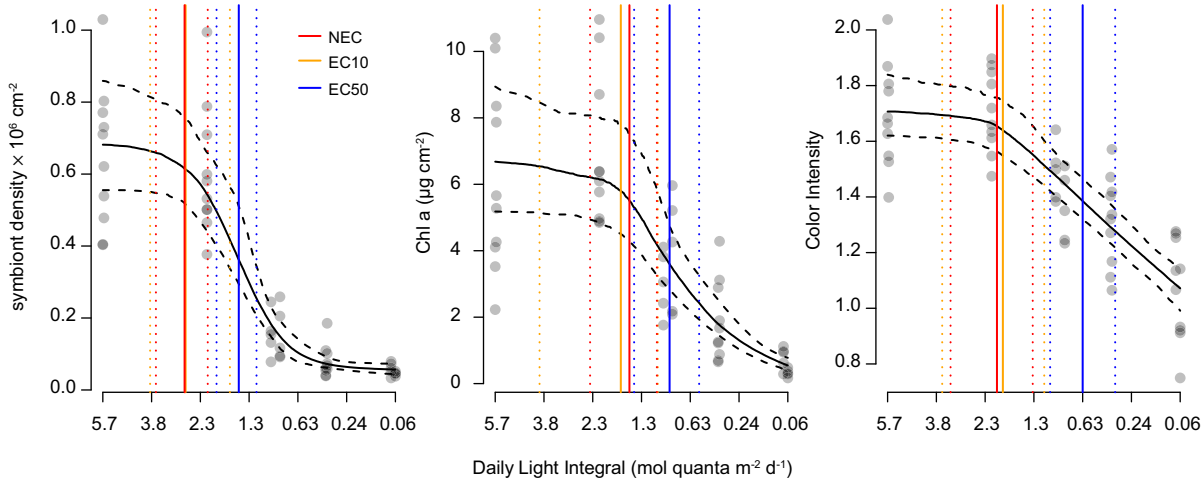


Fig. 8. Concentration response functions for *P. verrucosa* based on rescaled symbiont density, total Chl a content (µg cm^{-2}) and colour, based on the mean grey pixel intensity. The black solid line shows the fitted model and the solid, vertical red line the model averaged predicted No Effect Concentration (NEC) threshold values, vertical orange line the derived relative EC10 threshold values, and the vertical blue lines the derived relative EC50 threshold values, with 95% credible intervals for the model, NEC, EC10 and EC50 values indicated by dashed lines. Models fitted using the *jagsNEC* package in *R*, see methods. (For interpretation of the references to colour in this figure legend, the reader is referred to the web version of this article.)

interspersed with clement periods. The running means/percentiles analysis over multiple time periods was designed to examine this, showing that over very short, sub-hourly and hourly time frames very high turbidity (> 50 NTU) can occur, but these are not prolonged and average NTUs over a day or two were five times lower. The analysis, which was based on a 3-year dataset, also allows for contextualization of different time periods of high turbidity and light reduction in future monitoring (Fisher et al., 2015; Jones et al., 2015). For example, the laboratory-based experiments described below investigated the response to low light (with elevated SSCs) over a 28-d period and over a treatment range of ~6 to 0.06 mol photons m^{-2} day^{-1}. This range was equal or less than the 10th percentile (of low light periods) to lower than the 0th percentile over a 28-d period. That is, the lowest light reduction level used in the laboratory-based experiments was purposefully lower than anything measured on the reefs around Magnetic Island (in order to produce a dose-response relationship).

4.2. Laboratory-based exposure study

All corals and sponge species survived the 28-d experiment, with no mortality or even partial mortality observed; however, a range of sublethal effects were identified in all species including changes in colour, symbiont densities, pigment concentrations and lipid levels. One of the most consistent responses was the decrease in the ratio of storage to structural lipids with a reduction in light/increase in SSCs (see also Jones et al. (2020)). This can be directly attributed to a decrease in the storage lipids, wax ester and triacylglycerol, both of which account for 40–73% of the total lipids (Harland et al., 1993; Oku et al., 2002; Yamashiro et al., 1999) and constitute important energy reserves in corals (Imbs, 2013; Lin et al., 2013). Like the corals in the present study, an immediate reduction of triacylglycerol was identified after experimental and natural bleaching in *Porites compressa* and *M. verrucosa* (Grottoli et al., 2004; Rodrigues et al., 2008), as well as in *A. millepora* subjected to nutritional deficiency (Conlan et al., 2018). Although individual lipid classes were not analysed, the ratio of storage to structural lipids also decreased in the coral *A. nobilis* at a shallow turbid site and deep low light site (Saunders et al., 2005). This indicates that light is likely to be an important factor for lipid ratios as previously shown for total lipid composition, with a 30% reduction in light from the field to the experimental system during a three-week acclimation period contributing to a 30–50% drop in lipid content (Anthony et al., 2007). While the ratio of storage to structural lipids decreased for *C. orientalis* in the present study (driven by a decrease in triacylglycerol), no significant differences were observed in percent total lipids as light decreased and SSCs increased along the treatment range. This is consistent with previous work examining the effects of elevated SSCs on sponges that showed no significant difference in the percentage of total lipids in *C. orientalis* between 0, 30 and 100 mg L^{-1} (Pineda et al., 2017b).

The most sensitive taxon was the branching pocilloporid coral *P. verrucosa* which displayed the most noticeable changes in all response variables along the treatment range. This included a drop in the ratio of storage to structural lipids and total lipids, mirrored by a decrease in the number of algal symbionts causing the corals to change colour i.e., bleach. This dissociation of the symbiosis under similar light reduction levels has been recorded in *P. elegans* in 10–20 days (preceding death after 30 days) (Franzisket, 1970) and *Stylophora pistillata* also displayed signs of bleaching in darkness in a similar time frame of 10 d (Hoegh-Guldberg and Smith, 1989; Titlyanov et al., 2001). These species are all from the Pocilloporidae family which are generally regarded as phototropic species with small polyps and tentacles and reduced heterotrophic carbon acquisition capabilities (Einbinder et al., 2009; Wellington, 1982; Ziegler et al., 2014). This sensitivity to light reduction in the Pocilloporidae suggests that in the absence of other disturbance such as temperature, discolouration could be suitable as an early warning sign of light limitation during dredging programs (Jones et al., 2020), or coastal developments (Poquita-Du et al., 2019; Ziegler et al., 2014).

Overall, there is some evidence to suggest a difference in susceptibility to light reduction in corals between corals from clear-water (offshore), mid-shelf reefs of the GBR and those collected from the turbid zone communities. Using corals from a clear-water reef Bessell-Browne et al. (2017a) noted discolouration (bleaching) of *A. millepora*, *M. capricornis* and *Porites lutea/lobata* held in <1.1 mol photons m^{-2} d^{-1} for 30 days (in conjunction with elevated SSCs), and eventual partial mortality, especially in a darkness treatment. In another study with *A. millepora* and *P. acuta* corals collected from a clear-water reef and exposed to low light alone (in the absence of SSCs), Bessell-Browne et al. (2017b) reported paling after 10 d when exposed to <0.1 mol photons m^{-2} d^{-1} and by 20 days the corals were bone white. The corals exposed to 0.4 mol photons m^{-2} d^{-1} for 30 d also paled. In the most recent study, with corals also collected from a clear-water reef, discolouration and loss of algal symbionts was recorded *A. millepora*, *P. damicornis*, *Porites lutea/lobata* and *Turbinaria mesenterina* albeit after 42 d in darkness (with elevated SSCs). In the same experiment bleaching was observed in *P. damicornis* and *Porites lutea/lobata* in the 0.25 mol photons m^{-2} d^{-1} treatment for 30 days. The results from these previous studies with *P. acuta* and *P. damicornis* are comparable with our findings for *P. verrucosa*; however, the results for *A. millepora* are very different. We found that *A. millepora* (and *M. aequituberculata*) maintained algal densities even after 28 days in functional darkness (DLI of 0.06 mol quanta m^{-2} d^{-1}, administered in conjunction with sediments). A strict comparison among these studies is not possible because there were difference in the experimental setup beyond simply differences in the location from which the corals were collected including differences in the spectral qualities of the lights used, experimental durations and whether the experiments included elevated SSCs. Nevertheless, the ability of the turbid-zone *A. millepora* and *M. aequituberculata* corals in this study to maintain their algal compliment despite a month of darkness is notable. A possible explanation for this resilience is the buffering effect of an enhanced energy status and larger lipid store. The corals *Acropora valida* and *Turbinaria mesenterina* from turbid zone (coastal) reefs have a 2– and 4–times, respectively, higher lipid storage levels than from offshore (clear-water) reefs (Anthony, 2006). The difference is presumably aquired from higher rates of particulate feeding (Anthony, 2006), allowing the corals to endure longer periods of low light periods than clear-water conspecifics.

4.3. Risk assessing dredging and turbidity

To quantify the turbidity dose-response relationship statistical techniques commonly used in ecotoxicology and ecological risk assessment were used. These included determining no effect concentration (NEC) values (van der Hoeven et al., 1997) and effect concentration (EC10) values, both of which are preferred statistical estimates in Australia (Warne et al., 2015). Guideline values need to be developed with endpoints that are ecologically relevant such as lethality, growth etc. (Warne et al., 2015). We consider the sublethal dissociation of the symbiosis (bleaching, Douglas (2003)) the most ecologically relevant endpoint. The EC10 (and NEC) value for *P. verrucosa* were both ~2.7 mol photons m^{-2} d^{-1} over a 28-d or approximately 1-month time frame.

The probability of light reduction from natural resuspension events and/or dredging of the Sea Channel, with or without the shading effects of clouds, affecting corals on the reefs at Magnetic Island was assessed by comparing the 28-d EC10/NEC value from the laboratory studies to the 28-d running mean DLI values measured in-situ. The 28-d running mean DLI value was colour coded to indicate periods in the ranges of >5, 5–3, 3–2, 2–1 and <1 mol photons m^{-2} d^{-1} (Fig. 4). At sites A and B the 28-d running mean DLI never fell below the experimental 28-d EC10 (and NEC) value for *P. verrucosa*, but briefly fell into the 3–5 mol photons m^{-2} d^{-1} range on one occasion and at one site (site B, in June 2016) (Fig. 4C). This period coincided with 2 days of maintenance dredging in the Sea Channel and although elevated turbidity was detected it is not known whether the turbidity was caused by the dredging or due to natural wind

and/or waves resuspension. Irrespective of the cause, the pertinent point is that the period occurred (a) close to the winter solstice, (b) during cloudy days where there was less available surface light, and (c) after a spate of cloudy days in the previous weeks. All these factors would have contributed to the gradual lowering of the 28-d running mean DLI demonstrating the need to also consider ambient light including season and cloud cover with light-based monitoring programs.

Overall, at sites A and B light conditions seemed compatible with long-term survival of a light sensitive coral species, *P. verrucosa* at that location and depth in contrast to the much more turbid innermost shoal site (site C, Virago Shoal). At site C the 28-d running mean DLI at 4 m depth frequently fell below 3 mol photons m^2 d^{-1} (for ~15% of time) and even 2 mol photons m^2 d^{-1}. These values seem incompatible with long-term survivorship of *P. verrucosa* at that location and depth (5 m). Virago shoal is very depauperate of corals which, are typically limited to the upper 3 m. Although Pocilloporids have been seen at Virago Shoals in the shallows, the few coral species occurring on the shoal are composed of the turbid water specialists *Turbinaria mesenterina* (Jones et al., 2020) and encrusting Montipora, massive Porites or Faviids spp.

Over short periods of time i.e., days, occasional periods of very low light (or even darkness) are clearly tolerable by even highly phototropic coral species. This temporary light reduction could occur through the effects of clouds and suspended sediments (and water depth) acting alone or in combination. On such days corals may experience reduced or even negative energy balances i.e., light is a limiting factor (Anthony and Connolly, 2004; Anthony and Larcombe, 2000). In addition, catabolizing lipid stores may be one mechanism by which corals tolerate short-term deficits, potentially representing photoadaptation to low light (Anthony and Hoegh-Guldberg, 2003), when heterotrophic feeding is insufficient to compensate for the decline in photosynthesis that can occur in turbid-water habitats deeper than a few metres (Anthony, 2000; Anthony and Fabricius, 2000). Mobilizing and then replenishing energy reserves in clement (higher light) periods could be a mechanism by which turbid-zone coral communities could survive episodic short-term low light periods.

The 28-d running mean 2–3 mol photons m^{-2} d^{-1} value suggested here is conservative as it is based on a highly phototrophic coral. The guideline is also specific to the local inshore turbid-zone communities and specific to the local reef depth, but nevertheless a first attempt to integrate time and light reduction and spectral changes (in conjunction with sediments) into a parameter – 28-d running mean DLI – for risk assessing dredging and for monitoring during dredging projects. How extrapolatable these values are to other locations is difficult to evaluate at present because, as noted by Edmunds et al. (2018), there is so little empirically derived long-term information of light quantity (and quality) in coral reefs environments.

Although plumes of turbid water can be seen for tens of kilometers in some dredging projects, and are a powerful visual indicator of an environmental hazard, light reduction levels enough to represent a risk are an order of magnitude closer to the source (Bessell-Browne et al., 2017b; Jones et al., 2019a). The approaches used in this study can be used to more formally assess this. Measuring in-situ benthic light availability at frequent i.e., 10 min intervals, calculating daily light integrals and then calculating running mean DLIs is a suitable way to monitor and assess, at multiple time periods, the risk of light reduction from suspended sediments when dredging close to coral communities. In-situ monitoring programs providing telemetered data in real time during dredging can be incorporated into reactive management cascades to guide dredging operations once underway i.e., for deciding when, or if, to move a dredge to a different location or even stopping dredging.

CRediT authorship contribution statement

RJ and RF conceived of the study, HML, MCP, RF, RJ designed the experiments. HML and MCP conducted the experiments. RF and RJ analysed the water quality data. DSF conducted the lipid analyses. HML, GR and RF performed the statistical analyses. RJ wrote the first draft and HML, RF, MPC, GR, DSF contributed to the writing of the final draft. All authors approved the manuscript for submission.

Declaration of competing interest

None.

Acknowledgements

This project was funded by the Australian Government's National Environmental Science Programme (NESP Project 2.1.9) to RJ and RF. We acknowledge the Port of Townsville Limited (POTL) for access to the long-term water turbidity and light measurements in Cleveland Bay, for information on dredging volumes and locations, for access to the pilot boat and provision of crew for some of the field work, and for enabling and permitting close access to the dredge for sampling. We acknowledge Matt Salmon, Craig Humphrey, Andrea Severati, Paul Boyd and Eduardo Arias at the AIMS SeaSim for assistance with the design of the sediment dosing and lighting systems. We thank Annabel Smith-Moorhouse, Charlotte Harper, Maria Andersen and Zara Marks-Collins for their assistance with aquarium maintenance, sample processing and image analysis. The authors also acknowledge the Manbarra people as the Traditional Owners of the sea country where this work took place.

References

AIMS, 2020a. Australian Institute of Marine Science Northern Australia Automated Marine Weather and Oceanographic Stations, Sites: [Cape Bowling Green], Parameters: [light]. https://doi.org/10.25845/5c09bf93f315d. (Accessed 29 October 2020).

AIMS, 2020b. Australian Institute of Marine Science. Northern Australia Automated Marine Weather and Oceanographic Stations, Sites: (Cleveland Bay), Parameters: (light). https://doi.org/10.25845/5c09bf93f315d, accessed 29-Oct-2020.

Anthony, K., 2000. Enhanced particle-feeding capacity of coral on turbid reefs (Great Barrier Reef, Australia). Coral Reefs 19, 59–67. https://doi.org/10.1007/s003380050227.

Anthony, K., 2006. Enhanced energy status of corals on coastal, high-turbidity reefs. Mar. Ecol. Prog. Ser. 319, 111–116. https://doi.org/10.3354/meps319111.

Anthony, K., Connolly, S., 2004. Environmental limits to growth: physiological niche boundaries of corals along turbidity–light gradients. Oecologia 141, 373–384. https://doi.org/10.1007/s00442-004-1647-7.

Anthony, K., Fabricius, K., 2000. Shifting roles of heterotrophy and autotrophy in coral energetics under varying turbidity. J. Exp. Mar. Biol. Ecol. 252, 221–253. https://doi.org/10.1016/S0022-0981(00)00237-9.

Anthony, K., Hoegh-Guldberg, O., 2003. Kinetics of photoacclimation in corals. Oecologia 134, 23–31. https://doi.org/10.1007/s00442-002-1095-1.

Anthony, K., Larcombe, P., 2000. Coral reefs in turbid waters: sediment-induced stresses in corals and likely mechanisms of adaptation. In: Proceedings of the 9th International Coral Reef Symposium. Bali, Indonesia, 1, pp. 239–244.

Anthony, K., Ridd, P., Orpin, A., Larcombe, P., Lough, J., 2004. Temporal variation of light availability in coastal benthic habitats: effects of clouds, turbidity, and tides. Limnol. Oceanogr. 49, 2201–2211. https://doi.org/10.4319/lo.2004.49.6.2201.

Anthony, K., Connolly, S., Hoegh-Guldberg, O., 2007. Bleaching, energetics, and coral mortality risk: effects of temperature, light, and sediment regime. Limnol. Oceanogr. 52, 716–726. https://doi.org/10.4319/lo.2007.52.2.0716.

Bak, R.P.M., 1978. Lethal and sublethal effects of dredging on reef coral. Mar. Pollut. Bull. 9, 14–16. https://doi.org/10.1016/0025-326X(78)90275-8.

Bates, D., Mächler, M., Bolker, B., Walker, S., 2015. Fitting Linear Mixed-Effects Models Using lme4. 2015 67, p. 48. https://doi.org/10.18637/jss.v067.i01.

Bessell-Browne, P., Negri, A.P., Fisher, R., Clode, P.L., Duckworth, A., Jones, R., 2017a. Impacts of turbidity on corals: the relative importance of light limitation and suspended sediments. Mar. Pollut. Bull. 117, 161–170. https://doi.org/10.1016/j.marpolbul.2017.01.050.

Bessell-Browne, P., Negri, A.P., Fisher, R., Clode, P.L., Jones, R., 2017b. Impacts of light limitation on corals and crustose coralline algae. Sci. Rep. 7, 11553. https://doi.org/10.1038/s41598-017-11783-z.

Browne, N.K., 2012. Spatial and temporal variations in coral growth on an inshore turbid reef subjected to multiple disturbances. Mar. Environ. Res. 77, 71–83. https://doi.org/10.1016/j.marenvres.2012.02.005.

Browne, N.K., Smithers, S.G., Perry, C.T., 2010. Geomorphology and community structure of Middle Reef, central Great Barrier Reef, Australia: an inner-shelf turbid zone reef subject to episodic mortality events. Coral Reefs 29, 683–689. https://doi.org/10.1007/s00338-010-0640-3.

Browne, N.K., Smithers, S.G., Perry, C.T., Ridd, P.V., 2012. A field-based technique for measuring sediment flux on coral reefs: application to turbid reefs on the Great Barrier Reef. J. Coast. Res. 284, 1247–1262. https://doi.org/10.2112/jcoastres-d-11-00171.1.

Browne, N.K., Smithers, S.G., Perry, C.T., 2013. Spatial and temporal variations in turbidity on two inshore turbid reefs on the Great Barrier Reef, Australia. Coral Reefs 32, 195–210. https://doi.org/10.1007/s00338-012-0965-1.

Carter, R., Johnson, D., Hooper, K., 1993. Episodic post-glacial sea-level rise and the sedimentary evolution of a tropical continental embayment (Cleveland Bay, Great Barrier Reef shelf, Australia). Aust. J. Earth Sci. 40, 229–255. https://doi.org/10.1080/08120099308728077.

Ceccarelli, D.M., Evans, R.D., Logan, M., Mantel, P., Puotinen, M., Petus, C., Russ, G.R., Williamson, D.H., 2020. Long-term dynamics and drivers of coral and macroalgal cover on inshore reefs of the Great Barrier Reef Marine Park. Ecol. Appl. 30, e02008 https://doi.org/10.1002/eap.2008.

Conlan, J.A., Rocker, M.M., Francis, D.S., 2017. A Comparison of Two Common Sample Preparation Techniques for Lipid and Fatty Acid Analysis in Three Different Coral Morphotypes Reveals Quantitative and Qualitative Differences PeerJ 5:e3645. https://doi.org/10.7717/peerj.3645.

Conlan, J.A., Bay, L.K., Severati, A., Humphrey, C., Francis, D.S., 2018. Comparing the capacity of five different dietary treatments to optimise growth and nutritional composition in two scleractinian corals. PLoS One 13 (11), e0207956. https://doi.org/10.1371/journal.pone.0207956.

Cooper, T.F., Uthicke, S., Humphrey, C., Fabricius, K.E., 2007. Gradients in water column nutrients, sediment parameters, irradiance and coral reef development in the Whitsunday Region, central Great Barrier Reef. Estuar. Coast. Shelf Sci. 74, 458–470. https://doi.org/10.1016/j.ecss.2007.05.020.

Cooper, T.F., Ridd, P.V., Ulstrup, K.E., Humphrey, C., Slivkoff, M., Fabricius, K.E., 2008. Temporal dynamics in coral bioindicators for water quality on coastal coral reefs of the Great Barrier Reef. Mar. Freshw. Res. 59, 703–716. https://doi.org/10.1071/MF08016.

Done, T.J., 1982. Patterns in the distribution of coral communities across the central Great Barrier Reef. Coral Reefs 1, 95–107. https://doi.org/10.1007/bf00301691.

Douglas, A.E., 2003. Coral bleaching—how and why? Mar. Pollut. Bull. 46, 385–392. https://doi.org/10.1016/S0025-326X(03)00037-7.

Duckworth, A., Giofre, N., Jones, R., 2017. Coral morphology and sedimentation. Mar. Pollut. Bull. 125, 289–300. https://doi.org/10.1016/j.marpolbul.2017.08.036.

Dunne, R., 2010. Coral-list – NOAA's coral health and monitoring program (CHAMP) listserver for coral reef information and news. Odyssey PAR loggers. LOGGERS. Fri Sep 10 11:41:26 EDT 2010. https://coral.aoml.noaa.gov/pipermail/coral-list/2010-September/008896.html.

Edmunds, P.J., Tsounis, G., Boulon, R., Bramanti, L., 2018. Long-term variation in light intensity on a coral reef. Coral Reefs 37, 955–965. https://doi.org/10.1007/s00338-018-1721-y.

Einbinder, S., Mass, T., Brokovich, E., Dubinsky, Z., Erez, J., Tchernov, D., 2009. Changes in morphology and diet of the coral *Stylophora pistillata* along a depth gradient. Mar. Ecol. Prog. Ser. 381, 167–174. https://doi.org/10.3354/meps07908.

EPA, 2016. Technical Guidance - Environment Impact Assessment of Marine Dredging Proposals. Environmental Protection Authority (EPA), Western Australia, 26 pp. Available at. https://www.epa.wa.gov.au/policies-guidance/technical-guidance-environmental-impact-assessment-marine-dredging-proposals.

Fabricius, K.E., 2005. Effects of terrestrial runoff on the ecology of corals and coral reefs: review and synthesis. Mar. Pollut. Bull. 50, 125–146. https://doi.org/10.1016/j.marpolbul.2004.11.028.

Fearns, P., Dorji, P., Broomhall, M., Chedzey, H., Symonds, G., Mortimer, N., Branson, P., Contardo, S., Shimizu, K., Sun, C., 2019. Plume characterisation – field studies. Report of theme 3 – project 3.2.1, prepared for the dredging science node, Western Australian marine science institution, Perth, Western Australia, 300 pp. Available at. https://www.wamsi.org.au/dredging-science-node/dsn-reports.

Fisher, R., Stark, C., Ridd, P., Jones, R., 2015. Spatial patterns in water quality changes during dredging in tropical environments. PLoS One 10 (12), e0143309. https://doi.org/10.1371/journal.pone.0143309.

Fisher, R., Ricardo, G., Fox, D., 2020. Bayesian concentration-response modelling using jagsNEC. https://doi.org/10.5281/ZENODO.3966864.

Foster, T., Corcoran, E., Erftemeijer, P., Fletcher, C., Peirs, K., Dolmans, C., Smith, A., Yamamoto, H., Jury, M., 2010. Dredging and port construction around coral reefs. PIANC Environmental Commission, Report No. 108. ISBN 978-2-87223-177-5. Available at. http://www.pianc.org.

Fox, D.R., 2010. A Bayesian approach for determining the no effect concentration and hazardous concentration in ecotoxicology. Ecotoxicol. Environ. Saf. 73, 123–131. https://doi.org/10.1016/j.ecoenv.2009.09.012.

Franzisket, L., 1970. The atrophy of hermatypic reef corals maintained in darkness and their subsequent regeneration in light. Int. Rev. Gesamten Hydrobiol. Hydrogr. 55, 1–12. https://doi.org/10.1002/iroh.19700550102.

GBRMPA, 2012. The use of hydrodynamic numerical modelling for dredging projects in the Great Barrier Reef Marine Park, External Guidelines. August 2012. In: Great Barrier Reef Marine Park Authority. Townsville, Queensland, Australia, 8 pp.

Grottoli, A.G., Rodrigues, L.J., Juarez, C., 2004. Lipids and stable carbon isotopes in two species of Hawaiian corals, *Porites compressa* and *Montipora verrucosa*, following a bleaching event. Mar. Biol. 145, 621–631. https://doi.org/10.1007/s00227-004-1337-3.

Guest, J.R., Tun, K., Low, J., Vergés, A., Marzinelli, E.M., Campbell, A.H., Bauman, A.G., Feary, D.A., Chou, L.M., Steinberg, P.D., 2016. 27 years of benthic and coral community dynamics on turbid, highly urbanised reefs off Singapore. Sci. Rep. 6, 36260. https://doi.org/10.1038/srep36260.

Harland, A.D., Navarro, J.C., Spencer Davies, P., Fixter, L.M., 1993. Lipids of some Caribbean and Red Sea corals: total lipid, wax esters, triglycerides and fatty acids. Mar. Biol. 117, 113–117. https://doi.org/10.1007/BF00702469.

Hoegh-Guldberg, O., Smith, G.J., 1989. The effects of sudden changes in light, temperature and salinity on the population density and export of zooxanthellae from the reef corals *Seriatopora hysterix* and *Stylophora pistillata*. Mar. Ecol. Prog. Ser. 129, 279–303. https://doi.org/10.1016/0022-0981(89)90109-3.

Hopley, D., Parnell, K., Isdale, P., 1989. The Great Barrier Reef Marine Park: dimensions and regional patterns. Aust. Geogr. Stud. 27, 47–66. https://doi.org/10.1111/j.1467-8470.1989.tb00591.x.

Hothorn, T., Bretz, F., Westfall, P., 2008. Simultaneous inference in general parametric models. Biom. J. 50, 346–363. https://doi.org/10.1002/bimj.200810425.

Imbs, A.B., 2013. Fatty acids and other lipids of corals: composition, distribution, and biosynthesis. Russ. J. Mar. Biol. 39, 153–168. https://doi.org/10.1134/S1063074013030061.

Jones, R.J., 2008. Coral bleaching, bleaching-induced mortality, and the adaptive significance of the bleaching response. Mar. Biol. 154, 65–80. https://doi.org/10.1007/s00227-007-0900-0.

Jones, R., Fisher, R., Stark, C., Ridd, P., 2015. Temporal patterns in water quality from dredging in tropical environments. PLoS One 10 (10), e0137112. https://doi.org/10.1371/journal.pone.0137112.

Jones, R., Bessell-Browne, P., Fisher, R., Klonowski, W., Slivkoff, M., 2016. Assessing the impacts of sediments from dredging on corals. Mar. Pollut. Bull. 102, 9–29. https://doi.org/10.1016/j.marpolbul.2015.10.049.

Jones, R., Fisher, R., Bessell-Browne, P., 2019a. Sediment deposition and coral smothering. PLoS One 14, e0216248. https://doi.org/10.1371/journal.pone.0216248.

Jones, R., Fisher, R., Francis, D., Klonowski, W., Luter, H., Negri, A., Pineda, N., Ricardo, G., Slivkoff, M., Whinney, J., 2019b. Risk Assessing Dredging Activities in Shallow-water Mesophotic Reefs. Report to the National Environmental Science Program. Cairns, Reef and Rainforest Research Centre Limited, 74 pp, Available at. https://www.rrrc.org.au/nesp-twq-publications/.

Jones, R., Giofre, N., Luter, H.M., Neoh, T.L., Fisher, R., Duckworth, A., 2020. Responses of corals to chronic turbidity. Sci. Rep. 10, 4762. https://doi.org/10.1038/s41598-020-61712-w.

Kirk, J., 2010. Light and Photosynthesis in Aquatic Ecosystems, Third edition. Cambridge University Press, New York. https://doi.org/10.1017/CBO9781139168212. 649 pp. Online ISBN: 9781139168212.

Kleypas, J.A., 1996. Coral reef development under naturally turbid conditions: fringing reefs near Broad Sound, Australia. Coral Reefs 15, 153–167. https://doi.org/10.1007/BF01145886.

Larcombe, P., Woolfe, K.J., 1999. Terrigenous sediments as influences upon Holocene nearshore coral reefs, central Great Barrier Reef, Australia. Aust. J. Earth Sci. 46, 141–154. https://doi.org/10.1046/j.1440-0952.1999.00694.x.

Larcombe, P., Ridd, P., Prytz, A., Wilson, B., 1995. Factors controlling suspended sediment on inner-shelf coral reefs, Townsville, Australia. Coral Reefs 14, 163–171. https://doi.org/10.1007/BF00367235.

Larcombe, P., Costen, A., Woolfe, K.J., 2001. The hydrodynamic and sedimentary setting of nearshore coral reefs, central Great Barrier Reef shelf, Australia: Paluma Shoals, a case study. Sedimentology 48, 811–835. https://doi.org/10.1046/j.1365-3091.2001.00396.x.

LI-COR Biosciences, 2018. Comparison of quantum wensors with different spectra lsensitivities - Technical Note. https://www.licor.com/documents/oi26ib7eb6wm5y5u9ebv4b3jodm09tf9. (Accessed January 2019), p. 8.

Lin, C., Wang, L.-H., Meng, P.-J., Chen, C.-S., Tsai, S., 2013. Lipid content and composition of oocytes from five coral species: potential implications for future cryopreservation efforts. PLoS One 8, e57823. https://doi.org/10.1371/journal.pone.0057823.

Macdonald, R., Ridd, P., Whinney, J., Larcombe, P., Neil, D., 2013. Towards environmental management of water turbidity within open coastal waters of the Great Barrier Reef. Mar. Pollut. Bull. 74, 82–94. https://doi.org/10.1016/j.marpolbul.2013.07.026.

Mobley, C.D., 1994. Light and Water: Radiative Transfer in Natural Waters. Academic Press, San Diego, California. ISBN 10: 0125027508.

Morgan, K.M., Perry, C.T., Smithers, S.G., Johnson, J.A., Daniell, J.J., 2016. Evidence of extensive reef development and high coral cover in nearshore environments: implications for understanding coral adaptation in turbid settings. Sci. Rep. 6, 29616. https://doi.org/10.1038/srep29616.

Ogston, A.S., Storlazzi, C.D., Field, M.E., Presto, M.K., 2004. Sediment resuspension and transport patterns on a fringing reef flat, Molokai, Hawaii. Coral Reefs 23, 559–569. https://doi.org/10.1007/s00338-004-0415-9.

Oku, H., Yamashiro, H., Onaga, K., Iwasaki, H., Takara, K., 2002. Lipid distribution in branching coral *Montipora digitata*. Fish. Sci. 68, 517–522. https://doi.org/10.1046/j.1444-2906.2002.00456.x.

Orpin, A., Ridd, P., 2012. Exposure of inshore corals to suspended sediments due to wave-resuspension and river plumes in the central Great Barrier Reef: a reappraisal. Cont. Shelf Res. 47, 55–67. https://doi.org/10.1016/j.csr.2012.06.013.

Orpin, A., Ridd, P., Stewart, L., 1999. Assessment of the relative importance of major sediment transport mechanisms in the central Great Barrier Reef lagoon. Aust. J. Earth Sci. 46, 883–896. https://doi.org/10.1046/j.1440-0952.1999.00751.x.

Orpin, A., Ridd, P., Thomas, S., Anthony, K., Marshall, P., Oliver, J., 2004. Natural turbidity variability and weather forecasts in risk management of anthropogenic sediment discharge near sensitive environments. Mar. Pollut. Bull. 49, 602–612. https://doi.org/10.1016/j.marpolbul.2004.03.020.

Parrish, C.C., Bodennec, G., Gentien, P., 1996. Determination of glycoglycerolipids by Chromarod thin-layer chromatography with Iatroscan flame ionization detection. J. Chromatogr. A 741, 91–97. https://doi.org/10.1016/0021-9673(96)00147-1.

Perry, C.T., Larcombe, P., 2003. Marginal and non-reef-building coral environments. Coral Reefs 22, 427–432. https://doi.org/10.1007/s00338-003-0330-5.

Perry, C., Smithers, S., Gulliver, P., Browne, N., 2012. Evidence of very rapid reef accretion and reef growth under high turbidity and terrigenous sedimentation. Geology (Boulder) 40, 719–722. https://doi.org/10.1130/G33261.1.

Pineda, M.C., Strehlow, B., Duckworth, A., Doyle, J., Jones, R., Webster, N.S., 2016. Effects of light attenuation on the sponge holobiont- implications for dredging management. Sci. Rep. 6, 39038. https://doi.org/10.1038/srep39038.

Pineda, M.-C., Strehlow, B., Kamp, J., Duckworth, A., Jones, R., Webster, N.S., 2017a. Effects of combined dredging-related stressors on sponges: a laboratory approach using realistic scenarios. Sci. Rep. 7, 5155. https://doi.org/10.1038/s41598-017-05251-x.

Pineda, M.-C., Strehlow, B., Sternel, M., Duckworth, A., Jones, R., Webster, N.S., 2017b. Effects of suspended sediments on the sponge holobiont with implications for dredging management. Sci. Rep. 7, 4925. https://doi.org/10.1038/s41598-017-05241-z.

Poquita-Du, R.C., Quek, Z.B.R., Jain, S.S., Schmidt-Roach, S., Tun, K., Heery, E.C., Chou, L.M., Todd, P.A., Huang, D., 2019. Last species standing: loss of Pocilloporidae corals associated with coastal urbanization in a tropical city state. Mar. Biodivers. 49, 1727–1741. https://doi.org/10.1007/s12526-019-00939-x.

Ports Australia, 2014. Dredging and Australian Ports. Subtropical and Tropical Ports, Ports Australia, Sydney, NSW Australia, 102 pp. Available at. https://www.portsaustralia.com.au/.

Rodrigues, L.J., Grottoli, A.G., Pease, T.K., 2008. Lipid class composition of bleached and recovering *Porites compressa* Dana, 1846 and *Montipora capitata* Dana, 1846 corals from Hawaii. J. Exp. Mar. Biol. Ecol. 358, 136–143. https://doi.org/10.1016/j.jembe.2008.02.004.

Rogers, C.S., 1990. Responses of coral reefs and reef organisms to sedimentation. Mar. Ecol. Prog. Ser. 62, 185–202. https://doi.org/10.3354/meps062185.

Saunders, S.M., Radford, B., Bourke, S.A., Thiele, Z., Bech, T., Mardon, J., 2005. A rapid method for determining lipid fraction ratios of hard corals under varying sediment and light regimes. Environ. Chem. 2, 331–336. https://doi.org/10.1071/en05043.

Schneider, C.A., Rasband, W.S., Eliceiri, K.W., 2012. NIH image to ImageJ: 25 years of image analysis. Nat. Methods 9, 671–675. https://doi.org/10.1038/nmeth.2089.

Shaffer, J.M., Beaulieu, J.J., 2012. Calibration of the odysseyTM photosynthetic irradiance recorderTM for absolute irradiance measures. J. Freshw. Ecol. 27, 599–605.

Smith, R.C., Baker, K.S., 1981. Optical properties of the clearest natural waters (200-800 nm). Appl. Opt. 20, 177. https://doi.org/10.1364/AO.20.000177.

Stimson, J., Kinzie, R.A., 1991. The temporal release of zooxanthellae from the reef coral *Pocillopora damicornis* (Linnaeus) under nitrogen-enrichment and control conditions. J. Exp. Mar. Biol. Ecol. 153, 63–74. https://doi.org/10.1016/S0022-0981(05)80006-1.

Storlazzi, C.D., Jaffe, B.E., 2008. The relative contribution of processes driving variability in flow, shear, and turbidity over a fringing coral reef: West Maui, Hawaii. Estuar. Coast. Shelf Sci. 77, 549–564. https://doi.org/10.1016/j.ecss.2007.10.012.

Storlazzi, C.D., Ogston, A.S., Bothner, M.H., Field, M.E., Presto, M.K., 2004. Wave- and tidally-driven flow and sediment flux across a fringing coral reef: southern Molokai, Hawaii. Cont. Shelf Res. 24, 1397–1419. https://doi.org/10.1016/j.csr.2004.02.010.

Titlyanov, E.A., Titlyanova, T.V., Yamazato, K., van Woesik, R., 2001. Photo-acclimation dynamics of the coral *Stylophora pistillata* to low and extremely low light. J. Exp. Mar. Biol. Ecol. 263, 211–225. https://doi.org/10.1016/S0022-0981(01)00309-4.

van der Hoeven, N., Noppert, F., Leopold, A., 1997. How to measure no effect. Part I: towards a new measure of chronic toxicity in ecotoxicology. Introduction and workshop results. Environmetrics 8, 241–248. https://doi.org/10.1002/(SICI)1099-095X(199705)8:3<241::AID-ENV244>3.0.CO;2-7.

Verspecht, F., Pattiaratchi, C., 2010. On the significance of wind event frequency for particulate resuspension and light attenuation in coastal waters. Cont. Shelf Res. 30, 1971–1982. https://doi.org/10.1016/j.csr.2010.09.008.

Warne, M., Batley, G., van Dam, R., Chapman, J., Fox, D., Hickey, C., Stauber, J., 2015. Revised method for deriving Australian and New Zealand water quality guideline values for toxicants. In: Prepared for the Council of Australian Government's Standing Council on Environment and Water (SCEW). Information Technology and Innovation, Brisbane, Queensland, Department of Science, 43 pp.

Wellington, G., 1982. An experimental analysis of the effects of light and zooplankton on coral zonation. Oecologia 52, 311–320. https://doi.org/10.1007/BF00367953.

Whinney, J., Jones, R., Duckworth, A., Ridd, P., 2017. Continuous *in situ* monitoring of sediment deposition in shallow benthic environments. Coral Reefs 36, 521–533. https://doi.org/10.1007/s00338-016-1536-7.

Wood, S., 2006. Generalized additive models: An introduction with R. In: 392 pp. Boca Raton, Florida, USA, Chapman & Hall, ISBN 9781584884743.

Woolfe, K.J., Larcombe, P., 1998. Terrigenous sediment accumulation as a regional control on the distribution of reef carbonates. In: Camoin, G., Davies, P. (Eds.), Reefs and Carbonate Platforms in the Pacific and Indian Oceans, International Association of Sedimentologists (IAS) Special Publication, 25, pp. 295–310. https://doi.org/10.1002/9781444304879.ch16.

Woolfe, K.J., Larcombe, P., 1999. Terrigenous sedimentation and coral reef growth: a conceptual framework. Mar. Geol. 155, 331–345. https://doi.org/10.1016/S0025-3227(98)00131-5--.

Yamashiro, H., Oku, H., Higa, H., Chinen, I., Sakai, K., 1999. Composition of lipids, fatty acids and sterols in Okinawan corals. Comp. Biochem. Physiol. B: Biochem. Mol. Biol. 122, 397–407. https://doi.org/10.1016/S0305-0491(99)00014-0.

Zamoum, T., Furla, P., 2012. *Symbiodinium* isolation by NaOH treatment. J. Exp. Biol. 215, 3875. https://doi.org/10.1242/jeb.074955.

Ziegler, M., Roder, C.M., Büchel, C., Voolstra, C.R., 2014. Limits to physiological plasticity of the coral *Pocillopora verrucosa* from the central Red Sea. Coral Reefs 33, 1115–1129. https://doi.org/10.1007/s00338-014-1192-8.